

A new First-Order mixture integer-valued threshold autoregressive process based on binomial thinning and negative binomial thinning

Danshu Sheng¹, Dehui Wang^{1,*}, Liuquan Sun²

1. *School of Mathematics and Statistics, Liaoning University, Shenyang, China.*

2. *Institute of Applied Mathematics, Academy of Mathematics and Systems Science,
Chinese Academy of Sciences, Beijing 100190, China*

Abstract In this paper, we introduce a new first-order mixture integer-valued threshold autoregressive process, based on the binomial and negative binomial thinning operators. Basic probabilistic and statistical properties of this model are discussed. Conditional least squares (CLS) and conditional maximum likelihood (CML) estimators are derived and the asymptotic properties of the estimators are established. The inference for the threshold parameter is obtained based on the CLS and CML score functions. Moreover, the Wald test is applied to detect the existence of the piecewise structure. Simulation studies are considered, along with an application: the number of criminal mischief incidents in the Pittsburgh dataset.

Keywords: Threshold integer-valued autoregressive models; Mixture thinning operator; Parameter estimation; Wald test.

1 Introduction

Threshold time series model and its applications have had a very large influence on various fields of research since the groundbreaking works of [Tong \(1978, 1983\)](#). For instance, [Chen et al. \(2011\)](#) provide an overview of the development of threshold autoregression (TAR) models and their use in finance. The use of TAR in economics is mentioned in [Hansen \(2011\)](#). [Chan et al. \(2004\)](#) introduced the nonlinear TAR model and applied it to actuarial science for insurance product pricing. TAR models often involve piecewise linearization by dividing a complicated system into regimes according to some threshold, offering a somewhat simple method of fitting a complex system. In recent years, to capture the piecewise phenomenon of discrete-valued time series, [Wang et al. \(2014\)](#) introduced a self-excited threshold Poisson autoregressive (SETPAR) model and applied it to global major earthquake data. [Möller et al. \(2016\)](#) proposed a basic self-exciting

*Corresponding author: wangdehui@lnu.edu.cn

threshold binomial AR(1) model (SETBAR(1)) with values across a finite range of counts. Möller and Weiß (2015) presented a brief survey of threshold models for integer-valued time series with an infinite range and introduced two new models for the case of a finite range. Additionally, some academics have studied the following self-excited threshold integer-valued autoregressive (SETINAR) types models based on different thinning operators,

$$X_t = \begin{cases} \alpha_1 \circ X_{t-1} + Z_t, & X_{t-1} \leq r \\ \alpha_2 \circ X_{t-1} + Z_t, & X_{t-1} > r; \end{cases}$$

where $\{Z_t\}$ is a sequence of i.i.d. random variables. For example, based on the binomial thinning operator (“ \circ ”), Monteiro et al. (2012) presented an integer-valued self-exciting threshold autoregressive (SETINAR(2,1)) process, and based on the negative binomial thinning operator (“ $*$ ”), Yang et al. (2018) studied an integer-valued TAR procedure (NBTINAR(1)). The definitions of the binomial thinning operator “ \circ ” and the negative binomial thinning operator “ $*$ ” are defined in Definition 2.1-(ii) and (iii).

It is clear that when the integer-valued time series model is defined using thinning operators, the operator characteristics are important because they affect the statistical properties of the model. As introduced by Nastić et al. (2017), the negative binomial thinning operators, might be used to describe elements or random events that, by self-replication, influence other elements, cause other random events, or otherwise contribute to the overall thinning total by more than 1. Thus, the random number produced by $\alpha * X_{t-1}$ might theoretically be larger than X_{t-1} , and the “ $*$ ” operator is better suited for fitting time series data with significant volatility. Furthermore, in the case of the binomial thinning operator, since it is the sum of X_{t-1} Bernoulli random variables, it cannot generate a random number larger than X_{t-1} , which means that the binomial thinning operator’s contribution to X_t is less than X_{t-1} .

Note that the SETINAR models described above choose the same operator for both segments, but in practice, the operator may vary depending on the value of X_{t-1} . That is, when X_{t-1} is in a range, it contributes to X_t in the form of a binomial thinning operator. However, when it is not in this range, it may contribute to X_t as a negative binomial thinning operator. Precisely for this reason, herein, we define a new thinning operator as a mixture of the binomial and the negative binomial operator. Moreover, the mixing is self-excited, so it is very capable of handling the requirements of certain counting data. Likewise, there are a variety of real-life examples where these types of mixed thinning integer-valued threshold autoregressive (TINAR) models are more likely to be used than the TINAR models based only on one of these two thinning operators.

Consider the number of infectious illness cases that are confirmed each day. The following will happen if the infectious disease being studied has obvious disease characteristics, has a significant impact on people, and has an incubation period that is shorter than the counting interval, where the incubation period is the period of time between exposure to pathogenic microorganisms and the onset of obvious symptoms. The patient will be kept completely alone in the hospital, only being able to communicate with the attending physician. In this situation, it makes sense to explain the contribution of the number of confirmed cases at

time $t - 1$ (X_{t-1}) to the number of confirmed cases at time t (X_t) using the INAR(1) model based on the binomial thinning operator (Bi-INAR(1)). However, if there are more than a certain number of confirmed cases, the hospital will be unable to treat everyone, forcing the patients to self-isolate at home. Patients will likely interact with many individuals as a result of this loose isolation, which will increase infections and the transmission rate of the infectious disease. An INAR(1) model based on the negative binomial thinning operator (NB-INAR(1)) can be used to characterize the number of confirmed cases at time t .

Of course, there are also cases where the characteristics of the infectious diseases studied are not obvious, and when the number of patients is small, it may often go unnoticed. At this time, the infection tends to display a cross-infection pattern, and the number of infectious diseases can be described by the NB-INAR(1) model. However, with an increase in the number of confirmed cases, national or regional governments will pay greater attention, and they will develop a series of plans to reduce this cross-infection; thus, it is more reasonable to use the Bi-INAR(1) model to describe the number of patients.

Motivated by the aforementioned examples, we propose a new first-order mixture thinning (binomial thinning and negative binomial thinning) integer-valued threshold autoregressive (BiNB-MTTINAR(1)) process. For this, we initially give the definition of the BiNB-MTTINAR(1) model and study the statistical inference for the proposed model. Furthermore, considering that the model will appear different from the general SETINAR model when $\alpha_1 = \alpha_2$, we propose a new method to estimate the threshold parameter r , and present a new Wald test for conditional variance to detect the existence of the piecewise structure. Finally, from the application, we can also see that our proposed model is very competitive.

The paper is organized as follows: In Section 2, we introduce the BiNB-MTTINAR(1) process and discuss its basic probabilistic and statistical properties. In Section 3, we propose two estimation methods for estimating the model parameters and threshold value. We construct two Wald test statistics for conditional expectation and conditional variance parameters, respectively, to test the existence of the piecewise structure. In Section 4, some simulation results for the estimation methods, the size and power of Wald tests are presented. Real data example is given in Section 5. Some concluding remarks are given in Section 6. All proofs are postponed to the Appendix.

2 The BiNB-MTTINAR(1) model

We first introduce the definition of the BiNB-MTTINAR(1) process.

Definition 2.1. *The process $\{X_t\}$ is called BiNB-MTTINAR(1) process if X_t follows the recursion*

$$X_t = \begin{cases} \phi_1 \circ X_{t-1} + Z_{1,t}, & X_{t-1} \leq r \\ \phi_2 * X_{t-1} + Z_{2,t}, & X_{t-1} > r, \end{cases} \quad (2.1)$$

or

$$X_t = \begin{cases} \phi_2 * X_{t-1} + Z_{2,t}, & X_{t-1} \leq r \\ \phi_1 \circ X_{t-1} + Z_{1,t}, & X_{t-1} > r. \end{cases} \quad (2.2)$$

For convenience, we write the above two models by the symbol R as follows

$$X_t = (\phi_1 \circ X_{t-1} + Z_{1,t})I_{1,t}^R + (\phi_2 * X_{t-1} + Z_{2,t})I_{2,t}^R, \quad t \in \mathbb{Z}, \quad (2.3)$$

where

$$(i) \quad I_{1,t}^R = \begin{cases} I\{X_{t-1} \leq r\}, R = 0, \\ I\{X_{t-1} > r\}, R = 1, \end{cases} \quad \text{and} \quad I_{2,t}^R = 1 - I_{1,t}^R = \begin{cases} I\{X_{t-1} > r\}, R = 0, \\ I\{X_{t-1} \leq r\}, R = 1; \end{cases} \quad \text{That is, } R = 0 \text{ indicates} \\ \text{that BiNB-MTTINAR}(1) \text{ represents the process (2.1).}$$

(ii) the binomial thinning operator " $\phi_1 \circ$ ", proposed by [Steutel and Van Harn \(1979\)](#), is defined as $\phi_1 \circ X = \sum_{i=1}^X B_i$, where $\phi_1 \in (0, 1)$, $\{B_i\}$ is a sequence of i.i.d. Bernoulli random variables satisfying $P(B_i = 1) = 1 - P(B_i = 0) = \phi_1$, B_i is independent of X ;

(iii) the negative binomial thinning operator " $\phi_2 *$ ", proposed by [Ristić et al. \(2009\)](#), is defined as $\phi_2 * X = \sum_{i=1}^X W_i$, where $\phi_2 \in (0, 1)$, $\{W_i\}$ is a sequence of i.i.d. Geometric random variables with parameter $\frac{\phi_2}{1+\phi_2}$, W_i is independent of X ;

(iv) $\{Z_{1,t}\}$ is a sequence of i.i.d. Poisson distributed random variables with mean λ , $\{Z_{2,t}\}$ is a sequence of i.i.d. geometric distributed random variables with parameter $\frac{\lambda}{1+\lambda}$, $\lambda \in (0, \infty)$;

(v) For fixed t , $Z_{1,t}$ is assumed to be independent of $\phi_1 \circ X_{t-1}$ and X_{t-l} for all $l \geq 1$, $Z_{2,t}$ is assumed to be independent of $\phi_2 * X_{t-1}$ and X_{t-l} for all $l \geq 1$.

Note that compared with the traditional integer-valued threshold models, the condition $\phi_1 \neq \phi_2$ is not necessary, which can reflect a scenario where the variance of the two regimes is different but the mean is the same. We can give an example to illustrate this situation. For instance, viral data show that for some viruses, their own activity remains unaltered, which means that their probability of transmission is unaltered. This may also be regarded as their conditional expectation of transmission being unchanged. However, due to the increase in the number of patients, resulting in a series of external influences such as cross-infection and increased virus density in the air, the virus spread faster, that is, the volatility (conditional variance) increased. The BiNB-MTTINAR(1) model is more suited for simulation at this time. In the following Remark, how to select R in practice is discussed.

Remark 2.1. In practice, we are more likely to select the BiNB-MTTINAR(1) model with $R = 0$ if the variance difference between the two regimes is extremely large. This is due to the fact that the variance difference between the two regimes at $R = 0$ is greater than it is at $R = 1$ based on the definitions of thinning operators and Poisson, Geometric random variables.

Obviously, the BiNB-MTTINAR(1) model is Markovian, transition probabilities are very important when we consider the conditional maximum likelihood estimate for the proposed model. So we first give the

transition probabilities of the BiNB-MTTINAR(1) process as follows,

$$\begin{aligned}
P(i, j) &= P(X_t = j | X_{t-1} = i) \\
&= P((\phi_1 \circ X_{t-1} + Z_{1,t})I_{1,t}^R + (\phi_2 * X_{t-1} + Z_{2,t})I_{2,t}^R = j | X_{t-1} = i) \\
&= p_1(i, j, \phi_1, \lambda)I_{1,t}^R + p_2(i, j, \phi_2, \lambda)I_{2,t}^R,
\end{aligned} \tag{2.4}$$

where

$$\begin{aligned}
p_1(i, j, \phi_1, \lambda) &= \sum_{m=0}^{\min(i, j)} \binom{i}{m} e^{-\lambda} \frac{\lambda^{j-m}}{(j-m)!} \phi_1^m (1-\phi_1)^{i-m}, \\
p_2(i, j, \phi_2, \lambda) &= \sum_{m=0}^j \frac{\Gamma(i+m)}{\Gamma(i)\Gamma(m+1)} \frac{\phi_2^m}{(1+\phi_2)^{i+m}} \frac{\lambda^{j-m}}{(1+\lambda)^{j-m+1}}.
\end{aligned} \tag{2.5}$$

Next, we are ready to state that there exists a strictly stationary and ergodicity of the BiNB-MTTINAR(1) process satisfying Definition 2.1. Proofs of the following propositions are in the Appendix.

Proposition 2.1. *Let $\{X_t\}_{t \in \mathbb{Z}}$ be the process defined in Definition 2.1. Then $\{X_t\}_{t \in \mathbb{Z}}$ is an irreducible, aperiodic, and positive recurrent (and hence ergodic) Markov chain. Thus, there exists a strictly stationary process satisfying (2.3).*

Since the existence of the first three moments is a necessary condition for deriving the asymptotic properties of the parameter estimation in Sect. 3, and the moments and conditional moments are useful in obtaining the appropriate estimating equations for parameter estimation, we then give the following propositions. For simplicity in notation, we denote $E(I_{1,t}^R) = p_1 = q$, $E(I_{2,t}^R) = p_2 = 1 - q$, $\mu_1 := E(X_t | X_t \leq r)$, $\mu_2 := E(X_t | X_t > r)$, $\sigma_1^2 := \text{Var}(X_t | X_t \leq r)$, $\sigma_2^2 := \text{Var}(X_t | X_t > r)$, $\gamma_h^{(1)} := \text{Cov}(X_t, X_{t+h} | X_{t+h} \leq r)$, $\gamma_h^{(2)} := \text{Cov}(X_t, X_{t+h} | X_{t+h} > r)$, where $\gamma_0^{(s)} = [(\sigma_s^2 + \mu_s^2) - \mu_s E(X_t)]$, $s = 1, 2$.

Proposition 2.2. *Let $\{X_t\}$ be the process defined by Definition 2.1. Then $E(X_t^k) < \infty$ for $k = 1, 2, 3$.*

Proposition 2.3. *Let $\{X_t\}$ be the process defined by Definition 2.1. Then*

- (i) $E(X_t | X_{t-1}) = \phi_1 X_{t-1} I_{1,t}^R + \phi_2 X_{t-1} I_{2,t}^R + \lambda$;
- (ii) $\text{Var}(X_t | X_{t-1}) = (\phi_1(1-\phi_1)X_{t-1} + \lambda)I_{1,t}^R + (\phi_2(1+\phi_2)X_{t-1} + \lambda(1+\lambda))I_{2,t}^R$;
- (iii) $E(X_t) = q\phi_1\mu_1 + (1-q)\phi_2\mu_2 + \lambda$;
- (iv) $\text{Var}(X_t) = q[\phi_1^2\sigma_1^2 + \phi_1(1-\phi_1)\mu_1] + q(1-q)\phi_1^2\mu_1^2 + q\lambda + (1-q)[\phi_2^2\sigma_2^2 + \phi_2(1+\phi_2)\mu_2] + q(1-q)\phi_2^2\mu_2^2 + (1-q)\lambda(1+\lambda) - 2q(1-q)(\phi_1\mu_1 + \lambda)(\phi_2\mu_2 + \lambda)$;
- (v) $\text{Cov}(X_t, X_{t+h}) = \sum_{s=1}^2 \phi_s p_s \gamma_{h-1}^{(s)}$;
- (vi) $\rho(h) := \text{Corr}(X_t, X_{t+h}) = [\sum_{s=1}^2 \phi_s p_s \gamma_{h-1}^{(s)}] \setminus \text{Var}(X_t)$.

3 Parameters Estimation for the BiNB-MTTINAR(1) model

Suppose we have a series of observations $\{X_t\}_{t=1}^n$ generated from the BiNB-MTTINAR(1) process. We first estimate the parameter $\boldsymbol{\theta} = (\phi_1, \phi_2, \lambda)^\top$ using conditional least squares (CLS) and conditional maximum likelihood (CML) methods, the threshold parameter r is assumed to be known until Sect. 3.3 where we will propose two methods to handle the unknown r case. Later in Sect. 3.4, we will provide two Wald test statistics for conditional expectation and conditional variance parameters to check the nonlinearity of the data. All the proofs are presented in the Appendix.

3.1 CLS Estimation

Let $g(\boldsymbol{\theta}, X_{t-1}) = E(X_t|X_{t-1}) = \phi_1 X_{t-1} I_{1,t}^R + \phi_2 X_{t-1} I_{2,t}^R + \lambda$, then the CLS estimator $\hat{\boldsymbol{\theta}}_{CLS} := (\hat{\phi}_{1,CLS}, \hat{\phi}_{2,CLS}, \hat{\lambda}_{CLS})^\top$ of $\boldsymbol{\theta}$ is obtained by minimizing the sum of the squared deviations

$$Q(\boldsymbol{\theta}) := \sum_{t=1}^n (X_t - g(\boldsymbol{\theta}, X_{t-1}))^2 = \sum_{t=1}^n U_t^2(\boldsymbol{\theta}),$$

where

$$U_t(\boldsymbol{\theta}) = X_t - \phi_1 X_{t-1} I_{1,t}^R - \phi_2 X_{t-1} I_{2,t}^R - \lambda.$$

From the first partial derivative equal to 0, after some calculations, we obtain the CLS estimators closed-form expressions as follows

$$\begin{aligned} \hat{\phi}_{1,CLS} &= \frac{\left(n \sum_{t=1}^n I_{2,t}^R X_{t-1}^2 - \left(\sum_{t=1}^n I_{2,t}^R X_{t-1} \right)^2 \right) M_1 + \sum_{t=1}^n I_{1,t}^R X_{t-1} \left(\sum_{t=1}^n I_{2,t}^R X_{t-1} M_2 - \sum_{t=1}^n I_{2,t}^R X_{t-1}^2 M_3 \right)}{n \sum_{k=1}^2 \left(\sum_{t=1}^n I_{k,t}^R X_{t-1}^2 \right) - \left(\sum_{t=1}^n I_{1,t}^R X_{t-1} \right)^2 \sum_{t=1}^n I_{2,t}^R X_{t-1}^2 - \left(\sum_{t=1}^n I_{2,t}^R X_{t-1} \right)^2 \sum_{t=1}^n I_{1,t}^R X_{t-1}^2}, \\ \hat{\phi}_{2,CLS} &= \frac{\left(n \sum_{t=1}^n I_{1,t}^R X_{t-1}^2 - \left(\sum_{t=1}^n I_{1,t}^R X_{t-1} \right)^2 \right) M_2 + \sum_{t=1}^n I_{2,t}^R X_{t-1} \left(\sum_{t=1}^n I_{1,t}^R X_{t-1} M_1 - \sum_{t=1}^n I_{1,t}^R X_{t-1}^2 M_3 \right)}{n \sum_{k=1}^2 \left(\sum_{t=1}^n I_{k,t}^R X_{t-1}^2 \right) - \left(\sum_{t=1}^n I_{1,t}^R X_{t-1} \right)^2 \sum_{t=1}^n I_{2,t}^R X_{t-1}^2 - \left(\sum_{t=1}^n I_{2,t}^R X_{t-1} \right)^2 \sum_{t=1}^n I_{1,t}^R X_{t-1}^2}, \\ \hat{\lambda}_{CLS} &= \frac{\sum_{t=1}^n I_{1,t}^R X_{t-1}^2 \left(\sum_{t=1}^n I_{2,t}^R X_{t-1} M_3 - \sum_{t=1}^n I_{2,t}^R X_{t-1} M_2 \right) - \sum_{t=1}^n I_{1,t}^R X_{t-1} \sum_{t=1}^n I_{2,t}^R X_{t-1}^2 M_1}{n \sum_{k=1}^2 \left(\sum_{t=1}^n I_{k,t}^R X_{t-1}^2 \right) - \left(\sum_{t=1}^n I_{1,t}^R X_{t-1} \right)^2 \sum_{t=1}^n I_{2,t}^R X_{t-1}^2 - \left(\sum_{t=1}^n I_{2,t}^R X_{t-1} \right)^2 \sum_{t=1}^n I_{1,t}^R X_{t-1}^2}, \end{aligned} \quad (3.1)$$

where

$$M_1 = \sum_{t=1}^n X_t X_{t-1} I_{1,t}^R, \quad M_2 = \sum_{t=1}^n X_t X_{t-1} I_{2,t}^R, \quad M_3 = \sum_{t=1}^n X_t.$$

From Propositions 2.1 and 2.2, the BiNB-MTTINAR(1) model is stationary, ergodic, and the first three moments are bounded, it follows from Theorems 3.1 and 3.2 in Klimko and Nelson (1978) that $\hat{\boldsymbol{\theta}}_{CLS}$ is a consistent and asymptotically normal estimator of $\boldsymbol{\theta}$. That is, the following theorem about the consistency and asymptotic properties of the CLS estimator is valid.

Theorem 3.1. *Let $\{X_t\}$ be a BiNB-MTTINAR(1) process. Then the CLS estimator $\hat{\boldsymbol{\theta}}_{CLS}$ is consistent and has the asymptotically distribution,*

$$\sqrt{n}(\hat{\boldsymbol{\theta}}_{CLS} - \boldsymbol{\theta}_0) \xrightarrow{d} N(\mathbf{0}, \mathbf{V}^{-1} \mathbf{W} \mathbf{V}^{-1}), \quad (3.2)$$

where \mathbf{V} and \mathbf{W} are square matrices of order 3 with the ij th element given by

$$V_{ij} := E \left(\frac{\partial}{\partial \boldsymbol{\theta}_i} g(\boldsymbol{\theta}, X_{t-1}) \frac{\partial}{\partial \boldsymbol{\theta}_j} g(\boldsymbol{\theta}, X_{t-1}) \right)_{\boldsymbol{\theta}_0},$$

$$W_{ij} := E \left(U_t^2(\boldsymbol{\theta}) \frac{\partial}{\partial \boldsymbol{\theta}_i} g(\boldsymbol{\theta}, X_{t-1}) \frac{\partial}{\partial \boldsymbol{\theta}_j} g(\boldsymbol{\theta}, X_{t-1}) \right)_{\boldsymbol{\theta}_0}.$$

3.2 CML Estimation

For a fixed value of x_0 , the conditional likelihood function for the BiNB-MTTINAR(1) model can be written as

$$L(\boldsymbol{\theta}) := P(X_1 = x_1, \dots, X_n = x_n | x_0) = \prod_{t=1}^n P(x_{t-1}, x_t),$$

where $P(x_{t-1}, x_t)$ is the transition probabilities defined in (2.4). The CML estimator $\hat{\boldsymbol{\theta}}_{CML} := (\hat{\phi}_{1,CML}, \hat{\phi}_{2,CML}, \hat{\lambda}_{CML})^\top$ of $\boldsymbol{\theta}$ is obtained by maximizing the conditional log-likelihood function

$$\ell(\boldsymbol{\theta}) = \log L(\boldsymbol{\theta}) = \sum_{t=1}^n \ell_t(\boldsymbol{\theta}),$$

where $\ell_t(\boldsymbol{\theta}) = \log P(x_{t-1}, x_t)$.

Although no closed-form expressions for the estimators can be found, the numerical solutions can be solved by the MATLAB function `fmincon` or the R Function `optim` and the initial estimators required are obtained by the CLS estimators (3.1). The details of the numerical process are discussed later in Sect. 4. Next, we give the following theorem to state the consistency and asymptotic properties of the CML estimator.

Theorem 3.2. *Let $\{X_t\}$ be a BiNB-MTTINAR(1) process, then the CML estimator $\hat{\boldsymbol{\theta}}_{CML}$ is consistent and has the following asymptotically distribution,*

$$\sqrt{n}(\hat{\boldsymbol{\theta}}_{CML} - \boldsymbol{\theta}_0) \xrightarrow{d} N(\mathbf{0}, \mathbf{J}^{-1}(\boldsymbol{\theta}_0) \mathbf{I}(\boldsymbol{\theta}_0) \mathbf{J}^{-1}(\boldsymbol{\theta}_0)),$$

where $\mathbf{I}(\boldsymbol{\theta}_0) = E \left[\frac{\partial \ell_t(\boldsymbol{\theta})}{\partial \boldsymbol{\theta}} \frac{\partial \ell_t(\boldsymbol{\theta})}{\partial \boldsymbol{\theta}^\top} \right]_{\boldsymbol{\theta}_0}$, $\mathbf{J}(\boldsymbol{\theta}_0) = E \left[\frac{\partial^2 \ell_t(\boldsymbol{\theta})}{\partial \boldsymbol{\theta} \partial \boldsymbol{\theta}^\top} \right]_{\boldsymbol{\theta}_0}$.

3.3 Inference Method for Threshold r

In this section, we turn to the estimation of the threshold parameter r . Since r is an integer, the CLS and CML score functions are not differentiable with respect to r . As a result, the methods for selecting the

threshold r for integer-valued threshold models are primarily to search for the optimal value within a fixed interval $[r, \bar{r}]$ (typically using some empirical i th quantile value of the sample as a bound).

The methods commonly used at present can be divided into two groups. A straightforward approach is to multiply the threshold value r by the maximum $\ell(\boldsymbol{\theta})$ (see Wang et al. (2014)), i.e.

$$\hat{r}_{CML} = \arg \max_{r \in [r, \bar{r}]} \ell(\boldsymbol{\theta}). \quad (3.3)$$

Although this technique performs the best, the computational time is not ideal, especially for large sample size data since the CML score function's optimization speed is slow.

Another method of choosing threshold value is the minimum CLS score function $Q(\boldsymbol{\theta})$, see Möller et al. (2016), Li et al. (2018), i.e.

$$\hat{r}_{CLS}^{(1)} = \arg \min_{r \in [r, \bar{r}]} Q(\boldsymbol{\theta}).$$

Considering the computational speed and calculation burden, some researchers have provided algorithms for optimizing $\hat{r}_{CLS}^{(1)}$. For example, Li et al. (2018) proposed the doubly NeSS (D-NeSS) algorithm for the RCTINAR(1) process in view of Li and Tong (2016)'s nested subsample search (Ness) algorithm in the TAR model. The D-Ness algorithm is also applicable to the model we proposed, and the details of the D-Ness algorithm are provided in the Appendix.

It should be mentioned that the precondition for using the D-Ness algorithm is that the conditional expectations of two regimes are distinct, so the performance of $Q(\boldsymbol{\theta})$ is different for different threshold values r , i.e., $\phi_1 \neq \phi_2$ is needed. However, $\phi_1 \neq \phi_2$ is not necessary for the BiNB-MTTINAR(1) model. Considering this special case, we can choose the threshold r in the following way. It is worth noting that the conditional variance of the two regimes differs, i.e., there is no ϕ_1, ϕ_2, λ satisfying the following equation:

$$\phi_1(1 - \phi_1)X_{t-1} + \lambda = \phi_2(1 + \phi_2)X_{t-1} + \lambda(1 + \lambda),$$

for all $X_{t-1} \in \mathbb{N}_0$. Therefore, we can use the conditional variance as a criterion to select the threshold r . In view of the approach in Karlsen and Tjøstheim (1988) and Ristić et al. (2013), we choose the threshold r by minimizing the following score function:

$$\tilde{Q}_n(\boldsymbol{\theta}, r) = \sum_{t=1}^n (V_t - [\phi_1(1 - \phi_1)X_{t-1} + \lambda]I_{1,t}^R - [\phi_2(1 + \phi_2)X_{t-1} + \lambda(1 + \lambda)]I_{2,t}^R)^2, \quad (3.4)$$

where $V_t = (X_t - \phi_1 X_{t-1} I_{1,t}^R - \phi_2 X_{t-1} I_{2,t}^R - \lambda)^2$. Although this method can also get an estimator of the parameter $\boldsymbol{\theta}$, it does not perform as well as CLS estimator $\hat{\boldsymbol{\theta}}_{CLS}$ (3.1). So the estimation of $\boldsymbol{\theta}$ and r can be done in the following two steps:

Step1. For each $r \in [r, \bar{r}]$, find $\hat{r}_{CLS}^{(2)}$ such that

$$\hat{r}_{CLS}^{(2)} = \arg \min_{r \in [r, \bar{r}]} \tilde{Q}_n(\boldsymbol{\theta}, r). \quad (3.5)$$

Step2. $\hat{\boldsymbol{\theta}}_{CLS}$ is estimated by (3.1) under $r = \hat{r}_{CLS}^{(2)}$.

3.4 Wald Test

Threshold models are typically characterized by piecewise linearization by partitioning a complex system into regimes by some threshold. Therefore, a hypothesis test for detecting the existence of the piecewise structure is highly desirable. To date, many researchers have proposed different test statistics. A common and high-performance approach is to construct a likelihood ratio (LR) test based on the conditional likelihood function; see Möller et al. (2016). However, since the BiNB-MTTINAR(1) model is constructed by two operators, the LR test commonly used in TAR models cannot be effectively used to test the existence of a piecewise structure. Therefore, in our paper, we construct two Wald test statistics, also commonly used in threshold models, to detect the existence of the piecewise structure of the BiNB-MTTINAR(1) model.

3.4.1 Wald Test for Conditional Expectation parameters

The null hypothesis and the alternative hypothesis take the form:

$$H_0^{(1)} : \phi_1 = \phi_2 \quad \text{vs.} \quad H_1^{(1)} : \phi_1 \neq \phi_2.$$

That is, the existence of a piecewise structure is determined by checking whether the conditional expectation parameters are equal in two segment. A simple idea, learning from Yang and Li (2018), is to use the test of the difference between two normal population means based on the asymptotic normality of some consistent estimators. Then we construct the Wald test based on the asymptotically distribution (3.2) of the CLS estimator $\hat{\theta}_{CLS}$ and obtain the following result. That is

$$T_{Wald-E} = \frac{n(\hat{\phi}_1 - \hat{\phi}_2)^2}{\mathbf{\Lambda}_{11} + \mathbf{\Lambda}_{22} - \mathbf{\Lambda}_{12} - \mathbf{\Lambda}_{21}},$$

where $\mathbf{\Lambda} = \mathbf{V}^{-1} \mathbf{W} \mathbf{V}^{-1}$ and \mathbf{V}, \mathbf{W} are defined in Theorem 3.1. In fact, according to the ergodicity of the BiNB-MTTINAR(1) model, it is easy to see that $\hat{\mathbf{\Lambda}} = \hat{\mathbf{V}}^{-1} \hat{\mathbf{W}} \hat{\mathbf{V}}^{-1}$, where $\hat{\mathbf{V}}$ and $\hat{\mathbf{W}}$ given by

$$\hat{\mathbf{V}} = \begin{pmatrix} \frac{1}{n} \sum_{t=1}^n X_{t-1}^2 I_{1,t}^R & 0 & \frac{1}{n} \sum_{t=1}^n X_{t-1} I_{1,t}^R \\ 0 & \frac{1}{n} \sum_{t=1}^n X_{t-1}^2 I_{2,t}^R & \frac{1}{n} \sum_{t=1}^n X_{t-1} I_{2,t}^R \\ \frac{1}{n} \sum_{t=1}^n X_{t-1} I_{1,t}^R & \frac{1}{n} \sum_{t=1}^n X_{t-1} I_{2,t}^R & 1 \end{pmatrix},$$

$$\hat{\mathbf{W}} = \begin{pmatrix} \frac{1}{n} \sum_{t=1}^n U_t^2(\hat{\theta}) X_{t-1}^2 I_{1,t}^R & 0 & \frac{1}{n} \sum_{t=1}^n U_t^2(\hat{\theta}) X_{t-1} I_{1,t}^R \\ 0 & \frac{1}{n} \sum_{t=1}^n U_t^2(\hat{\theta}) X_{t-1}^2 I_{2,t}^R & \frac{1}{n} \sum_{t=1}^n U_t^2(\hat{\theta}) X_{t-1} I_{2,t}^R \\ \frac{1}{n} \sum_{t=1}^n U_t^2(\hat{\theta}) X_{t-1} I_{1,t}^R & \frac{1}{n} \sum_{t=1}^n U_t^2(\hat{\theta}) X_{t-1} I_{2,t}^R & \frac{1}{n} \sum_{t=1}^n U_t^2 \end{pmatrix},$$

$$U_t(\hat{\theta}) = X_t - \hat{\phi}_{1,CLS} X_{t-1} I_{1,t}^R - \hat{\phi}_{2,CLS} X_{t-1} I_{2,t}^R - \hat{\lambda}_{CLS},$$

are the consistent estimators of \mathbf{V} and \mathbf{W} (defined in Theorem 3.1). Thus

$$T_{Wald-E} = \frac{n(\hat{\phi}_1 - \hat{\phi}_2)^2}{\hat{\mathbf{\Lambda}}_{11} + \hat{\mathbf{\Lambda}}_{22} - \hat{\mathbf{\Lambda}}_{12} - \hat{\mathbf{\Lambda}}_{21}}, \quad (3.6)$$

then under $H_0^{(1)}$,

$$T_{Wald-E} \xrightarrow{d} \chi_1^2.$$

3.4.2 Wald Test for Conditional Variance parameters

As discussed in Sect. 3.3, checking $\phi_1 = \phi_2$ is not a complete indication that segmentation does not exist. After all, because the operators in the two segments are different, even the $\phi_1 = \phi_2$ segment structure still exists. This leads to a problem: T_{Wald-E} rejecting the null hypothesis can be used to justify that the piecewise structure exists, whereas T_{Wald-E} accepting the null hypothesis cannot be used to support the conclusion that the segmented structure does not exist. Considering this problem, we set the following null hypothesis and alternative hypothesis,

$$H_0^{(2)} : \sigma_1^2 = \sigma_2^2 \text{ and } b_1 = b_2 \quad \text{vs.} \quad H_1^{(2)} : \sigma_1^2 \neq \sigma_2^2 \text{ or } b_1 \neq b_2.$$

where $\sigma_1^2 = \text{Var}(B_i)$, $\sigma_2^2 = \text{Var}(W_i)$, $b_1 = \text{Var}(Z_{1,t})$, and $b_2 = \text{Var}(Z_{2,t})$. B_i and W_i are defined in Definition 2.1-(ii) and (iii). In order to construct test statistics, we first derive the CLS estimators and asymptotic distributions of the conditional variance.

Let $\boldsymbol{\vartheta} = (\sigma_1^2, \sigma_2^2, b_1, b_2)^\top$ be the conditional variance parameter vector,

$$g_1(\boldsymbol{\vartheta}, X_{t-1}) = \text{Var}(X_t | X_{t-1}) = (\sigma_1^2 X_{t-1} + b_1) I_{1,t}^R + (\sigma_2^2 X_{t-1} + b_2) I_{2,t}^R,$$

then the CLS estimator $\hat{\boldsymbol{\vartheta}} = (\hat{\sigma}_1^2, \hat{\sigma}_2^2, \hat{b}_1, \hat{b}_2)$ of $\boldsymbol{\vartheta}$ is obtained by minimizing the sum of the squared deviations,

$$\begin{aligned} S_n(\boldsymbol{\vartheta}) &= \sum_{t=1}^n D_t^2(\boldsymbol{\vartheta}) = \sum_{t=1}^n (V_t - g_1(\boldsymbol{\vartheta}, X_{t-1}))^2 \\ &= \sum_{t=1}^n (V_t - (\sigma_1^2 X_{t-1} + b_1) I_{1,t}^R - (\sigma_2^2 X_{t-1} + b_2) I_{2,t}^R)^2, \end{aligned}$$

where $V_t = \left(X_t - \hat{\phi}_{1,CLS} X_{t-1} I_{1,t}^R - \hat{\phi}_{2,CLS} X_{t-1} I_{2,t}^R - \hat{\lambda}_{CLS} \right)^2$, $\hat{\phi}_{1,CLS}$, $\hat{\phi}_{2,CLS}$ and $\hat{\lambda}_{CLS}$ are the CLS estimators from (3.1). Furthermore, $\hat{\boldsymbol{\vartheta}}$ is a consistent and asymptotically normal estimator of $\boldsymbol{\vartheta}$.

Theorem 3.3. *Let $\{X_t\}$ be a BiNB-MTTINAR(1) process, then the CLS estimator $\hat{\boldsymbol{\vartheta}}$ is consistent and has the following asymptotically distribution,*

$$\sqrt{n}(\hat{\boldsymbol{\vartheta}} - \boldsymbol{\vartheta}_0) \xrightarrow{d} N(\mathbf{0}, \boldsymbol{\Sigma}), \quad (3.7)$$

where $\boldsymbol{\Sigma} = \tilde{\mathbf{V}}^{-1} \tilde{\mathbf{W}} \tilde{\mathbf{V}}^{-1}$, $\tilde{\mathbf{V}}$ and $\tilde{\mathbf{W}}$ are square matrices of order 4 with the ij th element given by

$$\begin{aligned} \tilde{V}_{ij} &:= E \left(\frac{\partial}{\partial \boldsymbol{\vartheta}_i} g_1(\boldsymbol{\vartheta}, X_{t-1}) \frac{\partial}{\partial \boldsymbol{\vartheta}_j} g_1(\boldsymbol{\vartheta}, X_{t-1}) \right)_{\boldsymbol{\vartheta}_0}, \\ \tilde{W}_{ij} &:= E \left(D_t^2(\boldsymbol{\vartheta}) \frac{\partial}{\partial \boldsymbol{\vartheta}_i} g_1(\boldsymbol{\vartheta}, X_{t-1}) \frac{\partial}{\partial \boldsymbol{\vartheta}_j} g_1(\boldsymbol{\vartheta}, X_{t-1}) \right)_{\boldsymbol{\vartheta}_0}. \end{aligned}$$

Furthermore, Denote $\hat{\Sigma} = \hat{\mathbf{V}}^{-1} \hat{\mathbf{W}} \hat{\mathbf{V}}^{-1}$ and

$$\hat{\mathbf{V}} = \begin{pmatrix} \frac{1}{n} \sum_{t=1}^n X_{t-1}^2 I_{1,t}^R & 0 & \frac{1}{n} \sum_{t=1}^n X_{t-1} I_{1,t}^R & 0 \\ 0 & \frac{1}{n} \sum_{t=1}^n X_{t-1}^2 I_{2,t}^R & 0 & \frac{1}{n} \sum_{t=1}^n X_{t-1} I_{2,t}^R \\ \frac{1}{n} \sum_{t=1}^n X_{t-1} I_{1,t}^R & 0 & \frac{1}{n} \sum_{t=1}^n I_{1,t}^R & 0 \\ 0 & \frac{1}{n} \sum_{t=1}^n X_{t-1} I_{2,t}^R & 0 & \frac{1}{n} \sum_{t=1}^n I_{2,t}^R \end{pmatrix},$$

$$\hat{\mathbf{W}} = \begin{pmatrix} \frac{1}{n} \sum_{t=1}^n D_t^2(\hat{\boldsymbol{\theta}}) X_{t-1}^2 I_{1,t}^R & 0 & \frac{1}{n} \sum_{t=1}^n D_t^2(\hat{\boldsymbol{\theta}}) X_{t-1} I_{1,t}^R & 0 \\ 0 & \frac{1}{n} \sum_{t=1}^n D_t^2(\hat{\boldsymbol{\theta}}) X_{t-1}^2 I_{2,t}^R & 0 & \frac{1}{n} \sum_{t=1}^n D_t^2(\hat{\boldsymbol{\theta}}) X_{t-1} I_{2,t}^R \\ \frac{1}{n} \sum_{t=1}^n D_t^2(\hat{\boldsymbol{\theta}}) X_{t-1} I_{1,t}^R & 0 & \frac{1}{n} \sum_{t=1}^n D_t^2(\hat{\boldsymbol{\theta}}) I_{1,t}^R & 0 \\ 0 & \frac{1}{n} \sum_{t=1}^n D_t^2(\hat{\boldsymbol{\theta}}) X_{t-1} I_{2,t}^R & 0 & \frac{1}{n} \sum_{t=1}^n D_t^2(\hat{\boldsymbol{\theta}}) I_{2,t}^R \end{pmatrix},$$

$$D_t(\hat{\boldsymbol{\theta}}) = V_t - (\hat{\sigma}_1^2 X_{t-1} + \hat{b}_1) I_{1,t}^R - (\hat{\sigma}_2^2 X_{t-1} + \hat{b}_2) I_{2,t}^R,$$

$$V_t = (X_t - \hat{\phi}_{1,CLS} X_{t-1} I_{1,t}^R - \hat{\phi}_{2,CLS} X_{t-1} I_{2,t}^R - \hat{\lambda}_{CLS})^2.$$

Clearly, $\hat{\Sigma}$ is the consistent estimator of Σ . Then similar to the test statistics constructed in Sect. 3.4.1, we also use a test for the difference between two normal population means based on the asymptotic normality of the conditional variance parameter estimators. That is we construct the Wald test based on the asymptotically distribution (3.7) of the CLS estimator $\hat{\boldsymbol{\theta}}$ and obtain the following result. Define

$$T_{Wald-Var} = \frac{n(\hat{\sigma}_1^2 - \hat{\sigma}_2^2)^2}{\hat{\Sigma}_{11} + \hat{\Sigma}_{22} - \hat{\Sigma}_{12} - \hat{\Sigma}_{21}} + \frac{n(\hat{b}_1 - \hat{b}_2)^2}{\hat{\Sigma}_{33} + \hat{\Sigma}_{44} - \hat{\Sigma}_{34} - \hat{\Sigma}_{43}}, \quad (3.8)$$

Then under $H_0^{(2)}$,

$$T_{Wald-Var} \xrightarrow{d} \chi_2^2.$$

4 Simulation Studies

In this section, we first compare the performance of the proposed estimators under the case that r is known. Then, we investigate the performance of the threshold estimation methods proposed in Sect. 3.2. Finally, the empirical size and power of the Wald test are explored in Sect. 4.3.

Let us start by introducing the simulation study settings. The dataset $\{X_t\}_{t=1}^n$ is generated from the BiNB-MTTINAR(1) model (2.3): A1 - A4 (B1 - B4). The parameter settings are shown in Table 1. For each model, the value of r is chosen such that the observations in each regime comprise at least 20% of the total sample size. All simulations are conducted using MATLAB. The empirical results displayed in the tables and box plots, that is, the empirical biases and mean square errors (MSE), are computed over 10000 replications.

Table 1: Parameters setting of different models

Model	$R = 0$				Model	$R = 1$			
	ϕ_1	ϕ_2	λ	r		ϕ_1	ϕ_2	λ	r
A1	0.4	0.2	3	4	B1	0.4	0.2	3	4
A2	0.4	0.4	3	4	B2	0.4	0.4	3	4
A3	0.3	0.6	5	7	B3	0.3	0.6	5	7
A4	0.6	0.6	5	12	B4	0.6	0.6	5	12

Fig.1 shows the sample paths for Models A1 - B4 of the BiNB-MTTINAR(1) process and the mean and variance of the two regimes. Comparing the sample paths shown in Fig.1, we find that under the same parameter values, it is easier to distinguish the two regimes in the A1 - A4 models. This implies that when $R = 0$, distinguishing between the two regimes is easy. Meanwhile, by comparing the variance difference of the two regimes in the left and right halves of the figure, it can also be seen that, as discussed in Remark in Sect. 2, the variance difference between the two regimes of the BiNB-MTTINAR(1) model is more obvious when $R = 0$, especially when ϕ_2 is not less than ϕ_1 .

4.1 Simulation study when r is known

Table 2 and Table 3 report the bias and MSE of the CLS and CML estimators for Models A1 - B4 when r is known. The sample sizes considered are $n = 200, 500$ and 800 . From these two tables, it is easy to see that all the simulation results perform better as n increases, which implies that the two estimation methods can lead to good and consistent estimators when r is known. Moreover, $\hat{\theta}_{CML}$ has a smaller Bias and MSE, which implies that $\hat{\theta}_{CML}$ performs better than $\hat{\theta}_{CLS}$. Fig.2 is obtained from the bias of 10000 CLS and CML simulation estimators for Models A1 and B1. Note that the box plots are symmetric and centered on zero-bias, both bias and MSE for the CML estimators are smaller than the CLS estimators, which confirms the previous conclusions. Fig.3 shows the QQ plots of the CLS and CML estimators for Models A1 and B1 with sample size $n = 200$. From the QQ plots, we can see that the CLS and CML estimators are asymptotically normal for all parameters. Similar results are obtained for the remaining models, and the figures are omitted here to save space.

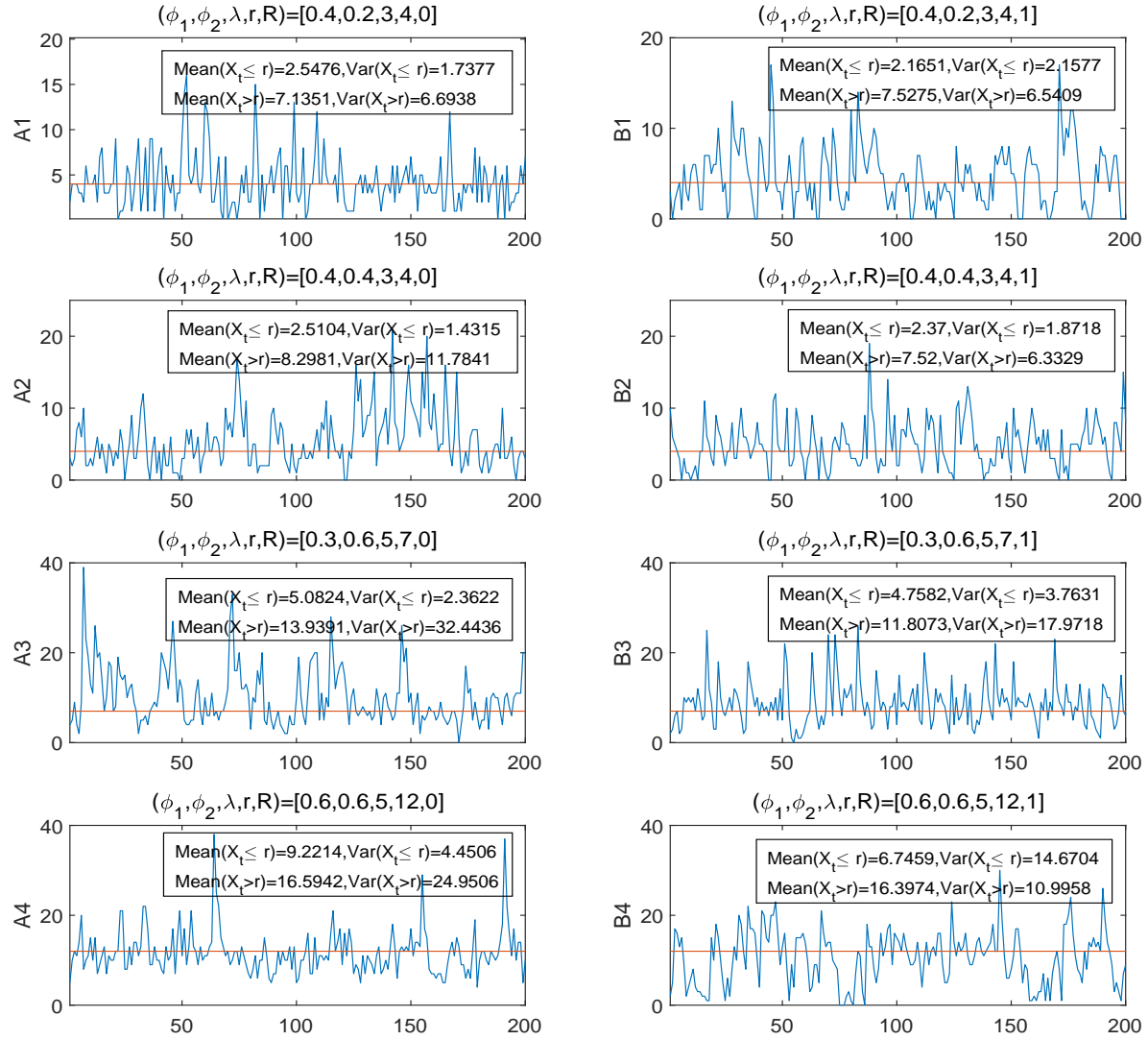


Fig. 1 Sample paths plots of models A1 - A4 and B1 - B4.

The red lines in the sample paths are the threshold values of each models.

Table 2: Simulation results for models A1 - B4 when r is known

n	Para.	A1				A2			
		CLS		CML		CLS		CML	
		Bias	MSE	Bias	MSE	Bias	MSE	Bias	MSE
200	ϕ_1	-0.0176	0.0235	0.0047	0.0113	-0.0269	0.0354	0.0023	0.0139
	ϕ_2	-0.0153	0.0070	0.0013	0.0025	-0.0199	0.0080	-0.0019	0.0029
	λ	0.0608	0.1932	-0.0125	0.0811	0.1050	0.3347	0.0007	0.1067
500	ϕ_1	-0.0090	0.0100	0.0017	0.0045	-0.0146	0.0149	0.0013	0.0053
	ϕ_2	-0.0069	0.0029	0.0007	0.0010	-0.0091	0.0032	-0.0009	0.0012
	λ	0.0310	0.0808	-0.0031	0.0323	0.0486	0.1346	-0.0027	0.0419
800	ϕ_1	-0.0043	0.0063	0.0007	0.0028	-0.0074	0.0095	0.0004	0.0033
	ϕ_2	-0.0037	0.0018	0.0001	0.0006	-0.0053	0.0020	-0.0008	0.0007
	λ	0.0138	0.0499	-0.0026	0.0191	0.0263	0.0856	0.0006	0.0263

n	Para.	A3				A4			
		CLS		CML		CLS		CML	
		Bias	MSE	Bias	MSE	Bias	MSE	Bias	MSE
200	ϕ_1	-0.0298	0.0348	0.0040	0.0133	-0.0175	0.0141	0.0037	0.0036
	ϕ_2	-0.0229	0.0068	-0.0031	0.0019	-0.0160	0.0066	0.0016	0.0017
	λ	0.2493	1.2945	-0.0072	0.3385	0.1783	1.1695	-0.0262	0.2748
500	ϕ_1	-0.0162	0.0169	0.0016	0.0052	-0.0073	0.0057	0.0017	0.0014
	ϕ_2	-0.0091	0.0026	-0.0010	0.0007	-0.0073	0.0027	0.0001	0.0007
	λ	0.1031	0.5114	-0.0032	0.1308	0.0740	0.4771	-0.0125	0.1094
800	ϕ_1	-0.0121	0.0110	0.0006	0.0033	-0.0043	0.0036	0.0012	0.0009
	ϕ_2	-0.0064	0.0016	-0.0008	0.0005	-0.0043	0.0017	0.0004	0.0004
	λ	0.0715	0.3241	-0.0018	0.0823	0.0443	0.2989	-0.0091	0.0680

Table 3: Simulation results for models B1 - B4 when r is known

n	Para.	B1				B2			
		CLS		CML		CLS		CML	
		Bias	MSE	Bias	MSE	Bias	MSE	Bias	MSE
200	ϕ_1	-0.0071	0.0050	0.0023	0.0026	-0.0075	0.0056	0.0029	0.0028
	ϕ_2	0.0104	0.0344	0.0140	0.0127	-0.0091	0.0477	0.0131	0.0193
	λ	0.0434	0.2559	-0.0250	0.1118	0.0491	0.3044	-0.0257	0.1345
500	ϕ_1	-0.0024	0.0020	0.0009	0.0010	-0.0029	0.0022	0.0011	0.0011
	ϕ_2	0.0002	0.0167	0.0047	0.0048	-0.0034	0.0209	0.0068	0.0073
	λ	0.0156	0.1032	-0.0090	0.0454	0.0169	0.1214	-0.0116	0.0528
800	ϕ_1	-0.0018	0.0012	-0.0001	0.0007	-0.0022	0.0014	0.0002	0.0007
	ϕ_2	-0.0004	0.0112	0.0022	0.0029	-0.0015	0.0128	0.0040	0.0045
	λ	0.0102	0.0632	-0.0018	0.0282	0.0129	0.0725	-0.0038	0.0321

n	Para.	B3				B4			
		CLS		CML		CLS		CML	
		Bias	MSE	Bias	MSE	Bias	MSE	Bias	MSE
200	ϕ_1	-0.0046	0.0057	0.0055	0.0025	-0.0117	0.0046	0.0002	0.0013
	ϕ_2	-0.0083	0.0422	0.0134	0.0129	-0.0129	0.0283	0.0075	0.0057
	λ	0.0518	0.8338	-0.0637	0.3060	0.1925	1.4799	-0.0204	0.3804
500	ϕ_1	-0.0022	0.0023	0.0020	0.0010	-0.0044	0.0017	-0.0002	0.0005
	ϕ_2	-0.0030	0.0173	0.0058	0.0049	-0.0058	0.0113	0.0021	0.0021
	λ	0.0226	0.3347	-0.0261	0.1206	0.0712	0.5467	-0.0045	0.1529
800	ϕ_1	-0.0010	0.0014	0.0015	0.0006	-0.0024	0.0010	0.0000	0.0003
	ϕ_2	-0.0016	0.0104	0.0035	0.0030	-0.0028	0.0073	0.0018	0.0013
	λ	0.0121	0.2022	-0.0170	0.0734	0.0371	0.3412	-0.0067	0.0950

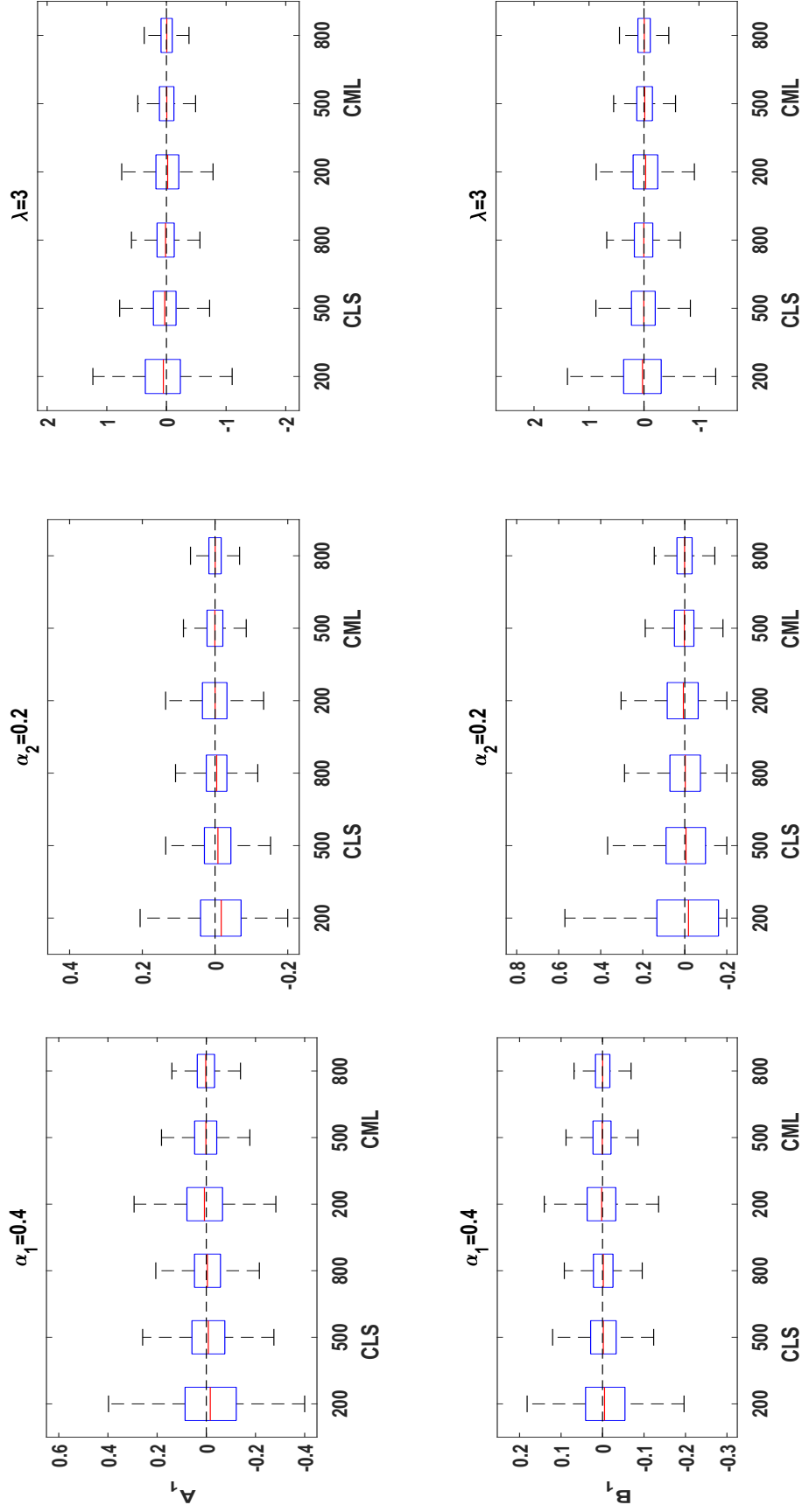


Fig. 2 Box plots from 10000 CLS and CML simulation estimators for models A1 and B1, sample size $n = 200, 500, 800$.

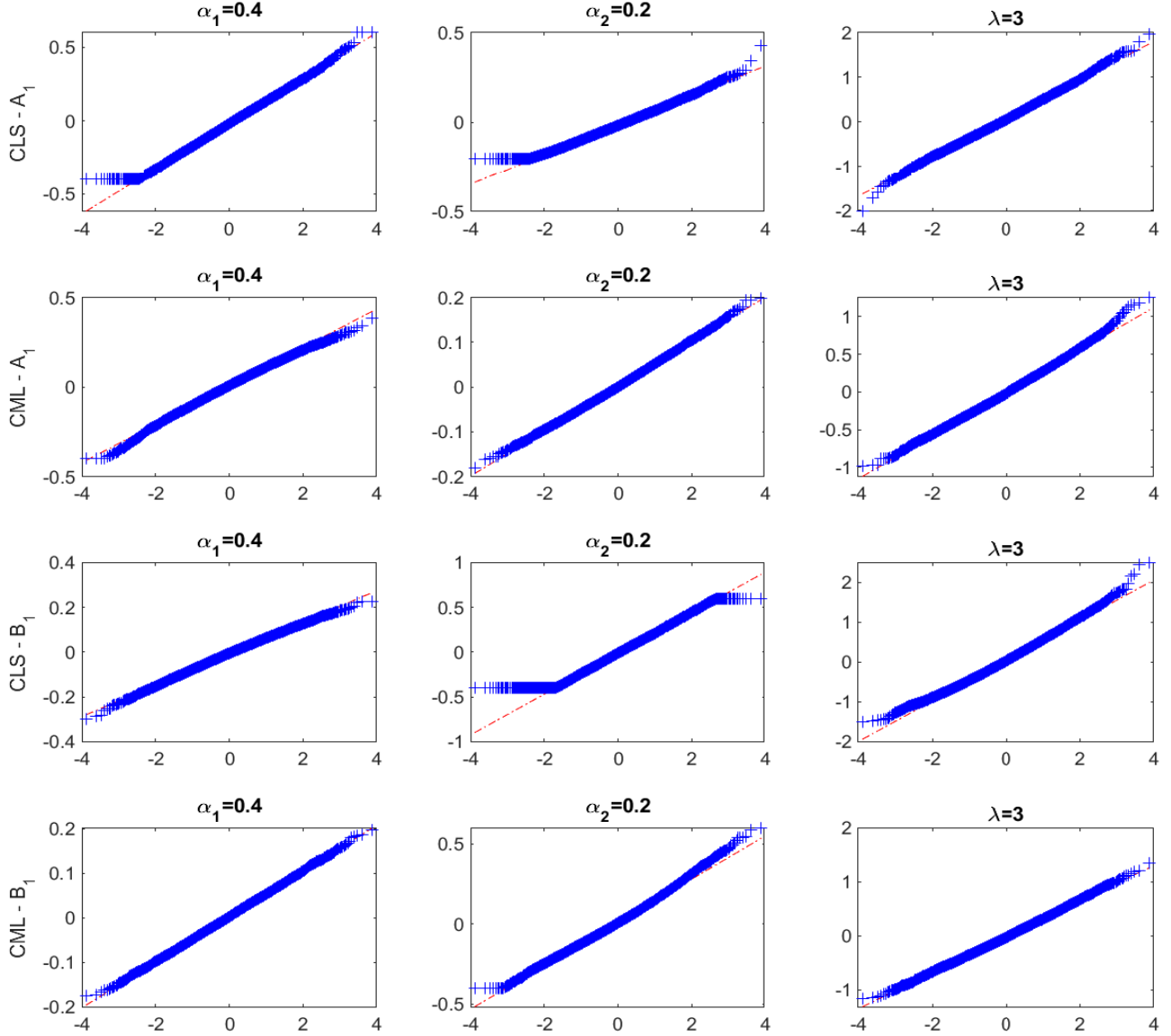


Fig. 3 QQ plots of CLS and CML estimators for models A1 and B1, sample size $n = 200$.

4.2 Simulation study under r is unknown

Table 4 and Table 5 report the bias and MSE of the CLS and CML estimators proposed in Set. 3.3 for Models A1 - B4. The considered sample sizes are $n = 200, 500, 800$ and 1500 . The search range of the threshold (i.e., $[r, \bar{r}]$) is set to the empirical 10th and 90th quantile of $\{X_t\}_{t=1}^n$. From these two tables, it is clear that both the bias and MSE of the CML estimators are very small, as expected. For the CLS estimators, where r is estimated by $r_{CLS}^{(2)}$, although their bias and MSE are larger than those of the CML estimators, they both

decrease with the increase of n . That is, both methods are reliable, which ensures that we can confidently use the BiNB-MTTINAR(1) model without worrying about incorrect results when r is unknown. A detailed explanation and analysis of threshold estimators are presented in Table 6.

Table 4: Simulation results for models A1 - A4 when r is unknown

n	Para.	A1				A2			
		CLS		CML		CLS		CML	
		Bias	MSE	Bias	MSE	Bias	MSE	Bias	MSE
200	ϕ_1	-0.1195	0.0486	0.0042	0.0116	-0.0423	0.0327	-0.0005	0.0154
	ϕ_2	-0.0268	0.0088	0.0008	0.0025	-0.0228	0.0090	-0.0040	0.0030
	λ	0.2809	0.3292	-0.0096	0.0820	0.1488	0.3160	0.0088	0.1142
	r	1.1117	4.1479	0.0133	0.0329	1.6532	8.5216	0.0399	0.1349
500	ϕ_1	-0.0731	0.0249	0.0019	0.0044	-0.0257	0.0141	0.0016	0.0052
	ϕ_2	-0.0147	0.0037	0.0012	0.0010	-0.0090	0.0034	-0.0008	0.0011
	λ	0.1597	0.1437	-0.0052	0.0320	0.0811	0.1278	-0.0031	0.0406
	r	0.5716	1.9082	0.0001	0.0001	0.8042	4.1302	0.0012	0.0020
800	ϕ_1	-0.0479	0.0156	0.0011	0.0028	-0.0163	0.0095	0.0008	0.0033
	ϕ_2	-0.0105	0.0022	0.0002	0.0006	-0.0063	0.0021	-0.0007	0.0007
	λ	0.1051	0.0894	-0.0024	0.0204	0.0511	0.0850	-0.0018	0.0252
	r	0.3502	1.1574	0	0	0.4330	2.1804	0.0001	0.0001
1500	ϕ_1	-0.0208	0.0071	0.0002	0.0015	-0.0092	0.0050	0.0003	0.0017
	ϕ_2	-0.0049	0.0011	0.0003	0.0003	-0.0041	0.0011	-0.0004	0.0004
	λ	0.0452	0.0419	-0.0006	0.0106	0.0301	0.0454	0.0011	0.0137
	r	0.1370	0.3988	0	0	0.1195	0.5153	0	0
n	Para.	A3				A4			
		CLS		CML		CLS		CML	
		Bias	MSE	Bias	MSE	Bias	MSE	Bias	MSE
200	ϕ_1	0.0788	0.0649	0.0048	0.0151	-0.0630	0.0258	0.0003	0.0040
	ϕ_2	-0.0058	0.0063	-0.0035	0.0019	-0.0360	0.0084	-0.0051	0.0021
	λ	-0.0675	1.5726	0.0010	0.3626	0.6224	2.2781	0.0086	0.3199
	r	2.2616	20.6480	0.0038	0.1084	2.0816	15.9816	0.0320	0.0970
500	ϕ_1	0.0249	0.0262	0.0020	0.0054	-0.0344	0.0100	0.0006	0.0014
	ϕ_2	-0.0033	0.0027	-0.0015	0.0007	-0.0154	0.0032	-0.0014	0.0008
	λ	-0.0021	0.5952	-0.0040	0.1375	0.3270	0.8893	-0.0027	0.1181
	r	0.7692	6.6242	-0.0010	0.0036	1.0950	9.0246	0.0008	0.0020
800	ϕ_1	0.0063	0.0159	0.0003	0.0033	-0.0228	0.0064	0.0006	0.0009
	ϕ_2	-0.0038	0.0017	-0.0007	0.0005	-0.0105	0.0021	-0.0006	0.0005
	λ	0.0362	0.3725	0.0038	0.0848	0.2177	0.5653	-0.0006	0.0741
	r	0.3615	3.0955	-0.0002	0.0002	0.6005	4.7813	0.0002	0.0002
1500	ϕ_1	-0.0024	0.0069	0	0.0017	-0.0102	0.0032	0.0001	0.0005
	ϕ_2	-0.0027	0.0009	-0.0004	0.0002	-0.0055	0.0011	-0.0006	0.0003
	λ	0.0317	0.1857	0.0030	0.0444	0.0956	0.2897	-0.0007	0.0395
	r	0.0702	0.5684	0	0	0.2046	1.5148	0	0

Table 5: Simulation results for models B1 - B4 when r is unknown

n	Para.	B1				B2			
		CLS		CML		CLS		CML	
		Bias	MSE	Bias	MSE	Bias	MSE	Bias	MSE
200	ϕ_1	0.0266	0.0053	0.0028	0.0026	0.0125	0.0053	0.0029	0.0029
	ϕ_2	0.2709	0.1771	0.0174	0.0136	0.1612	0.1103	0.0159	0.0212
	λ	-0.3076	0.3341	-0.0281	0.1159	-0.1382	0.2822	-0.0312	0.1412
	r	-1.1210	2.4938	0.0225	0.0899	-0.9897	2.1701	0.0146	0.1232
500	ϕ_1	0.0185	0.0023	0.0009	0.0010	0.0056	0.0021	0.0005	0.0011
	ϕ_2	0.1733	0.0944	0.0060	0.0049	0.0806	0.0524	0.0050	0.0071
	λ	-0.2134	0.1603	-0.0079	0.0454	-0.0615	0.1106	-0.0061	0.0522
	r	-0.8806	1.8220	0.0006	0.0008	-0.7650	1.6374	0	0.0030
800	ϕ_1	0.0148	0.0015	0.0007	0.0006	0.0045	0.0013	0.0004	0.0007
	ϕ_2	0.1327	0.0635	0.0040	0.0030	0.0598	0.0330	0.0038	0.0045
	λ	-0.1755	0.1101	-0.0069	0.0273	-0.0480	0.0719	-0.0045	0.0328
	r	-0.7371	1.4397	0	0	-0.6154	1.2624	0	0
1500	ϕ_1	0.0105	0.0009	0.0002	0.0003	0.0026	0.0007	0.0003	0.0004
	ϕ_2	0.0883	0.0343	0.0026	0.0016	0.0305	0.0150	0.0024	0.0024
	λ	-0.1277	0.0680	-0.0035	0.0148	-0.0274	0.0373	-0.0038	0.0174
	r	-0.5483	0.9755	0	0	-0.4118	0.7958	0	0
n	Para.	B3				B4			
		CLS		CML		CLS		CML	
		Bias	MSE	Bias	MSE	Bias	MSE	Bias	MSE
200	ϕ_1	-0.0104	0.0064	0.0048	0.0026	0.0201	0.0046	0.0013	0.0014
	ϕ_2	0.0102	0.0602	0.0131	0.0132	0.1237	0.0528	0.0062	0.0065
	λ	0.2001	1.0179	-0.0587	0.3162	-0.4410	1.3909	-0.0414	0.3708
	r	-0.9741	2.7825	-0.0062	0.0780	-2.3478	11.9148	-0.0061	0.0979
500	ϕ_1	-0.0107	0.0030	0.0019	0.0010	0.0104	0.0019	0.0004	0.0006
	ϕ_2	-0.0238	0.0320	0.0059	0.0050	0.0713	0.0239	0.0029	0.0024
	λ	0.1927	0.5398	-0.0217	0.1217	-0.2285	0.5555	-0.0138	0.1420
	r	-0.6208	1.7522	-0.0002	0.0014	-1.8164	8.4670	-0.0004	0.0026
800	ϕ_1	-0.0082	0.0020	0.0011	0.0006	0.0072	0.0011	0.0003	0.0003
	ϕ_2	-0.0241	0.0210	0.0028	0.0030	0.0475	0.0130	0.0021	0.0015
	λ	0.1456	0.3621	-0.0152	0.0742	-0.1610	0.3399	-0.0113	0.0867
	r	-0.4249	1.1403	0	0	-1.4694	6.4754	0	0
1500	ϕ_1	-0.0045	0.0010	0.0004	0.0003	0.0037	0.0006	0	0.0002
	ϕ_2	-0.0145	0.0110	0.0017	0.0016	0.0239	0.0057	0.0007	0.0008
	λ	0.0755	0.1913	-0.0068	0.0403	-0.0841	0.1812	-0.0019	0.0463
	r	-0.1935	0.5023	0	0	-0.9999	4.0159	0	0

Table 6 shows the D-Ness algorithm and the two estimation method performances of \hat{r} for Models A1 - B4, including the mean, the percentage of correctly identifying r ($CP(r)$) across 10000 replications and duration(s), that is, the computing time in seconds. For the D-Ness algorithm, we set $(\underline{\lambda}, \bar{\lambda}, L) = (2, 6, 4)$. Below, we will compare the three methods in terms of $CP(r)$ and duration(s).

In term of the percentage chance of correctly identifying r , there is no doubt that the advantage of \hat{r}_{CML} is particularly obvious. In particular, $CP(r)$ is above 0.9 with small sample size ($n = 200$) for all models. For the results of $\hat{r}_{CLS}^{(2)}$, although the correct percentage is not high when the sample size is small, it can also reach more than 0.9 (when $R = 0$) as the sample size increases ($n = 1500$). For $R = 1$, simulations show that when the sample size reaches 4000, $CP(r)$ can also reach 0.9. To save space, the details are not displayed in the table. At the same time, it is noted that the $CP(r)$ of $\hat{r}_{CLS}^{(2)}$ when $R = 1$ is obviously not as good as when $R = 0$, which is mainly because the variance difference between the two regimes is not as large as when $R = 0$, especially for Model B4, which also explains why the result of threshold estimation for Model B4 is not ideal. The result of the D-Ness algorithm shows that its performance in Models A2 and A4

Table 6: The performances of \hat{r} for models A1 - B4

Model	n	D-Ness			CLS estimator $\hat{r}_{CLS}^{(2)}$			CML estimator \hat{r}_{CML}		
		Mean	CP(r)	Duration(s)	Mean	CP(r)	Duration(s)	Mean	CP(r)	Duration(s)
A1	200	4.7590	0.4443	2.9870	5.1117	0.5231	1044.5860	4.0133	0.9826	3504.3890
	500	4.4779	0.6627	3.5810	4.5716	0.7100	1303.9650	4.0001	0.9999	7768.6120
	800	4.2766	0.8043	4.7590	4.3502	0.8148	1535.6430	4.0000	1.0000	13009.4190
	1500	4.0912	0.9362	5.9880	4.1370	0.9196	1359.1520	4.0000	1.0000	20730.0420
A2	200	5.7958	0.1440	3.1470	5.6532	0.4444	1251.7120	4.0399	0.9470	4650.2890
	500	5.5725	0.1948	4.2800	4.8042	0.6927	1730.1670	4.0012	0.9980	10875.8460
	800	5.4216	0.2337	4.5590	4.4330	0.8204	1506.4450	4.0001	0.9999	16219.0090
	1500	5.2820	0.2696	10.8690	4.1195	0.9403	2886.6380	4.0000	1.0000	34187.4860
A3	200	13.5680	0.1185	10.8900	9.2616	0.4839	5472.8070	7.0038	0.9236	29578.2180
	500	12.8048	0.2679	9.0360	7.7692	0.7708	3700.9410	6.9990	0.9964	61768.0290
	800	12.3470	0.3544	13.0000	7.3615	0.8759	4452.3240	6.9998	0.9998	103513.5660
	1500	11.4760	0.4820	15.7860	7.0702	0.9701	3738.1580	7.0000	1.0000	178727.1130
A4	200	15.0163	0.1129	5.5600	14.0816	0.4582	2890.8690	12.0320	0.9489	24881.2080
	500	14.7580	0.1382	7.4260	13.0950	0.6924	3257.2870	12.0008	0.9980	63494.5690
	800	14.8073	0.1367	9.9120	12.6005	0.8039	3829.1370	12.0002	0.9998	105284.7910
	1500	14.6125	0.1567	11.5210	12.2046	0.9230	2939.0570	12.0000	1.0000	175887.6020
Model	n	D-Ness			CLS estimator $\hat{r}_{CLS}^{(2)}$			CML estimator \hat{r}_{CML}		
		Mean	CP(r)	Duration(s)	Mean	CP(r)	Duration(s)	Mean	CP(r)	Duration(s)
B1	200	3.7723	0.5411	4.8820	2.8790	0.3895	1723.3820	4.0225	0.9696	6518.4220
	500	3.8636	0.7495	8.1240	3.1194	0.4834	2661.0870	4.0006	0.9992	16627.9210
	800	3.9045	0.8526	9.6060	3.2629	0.5378	2685.2930	4.0000	1.0000	25904.2070
	1500	3.9507	0.9375	11.4370	3.4517	0.6242	2313.6080	4.0000	1.0000	40997.9390
B2	200	3.7774	0.2547	3.1480	3.0103	0.4506	1016.0670	4.0146	0.9368	5479.4990
	500	3.9586	0.2752	3.9030	3.2350	0.5646	1099.0420	4.0000	0.9970	12834.6300
	800	4.0485	0.2899	6.0270	3.3846	0.6339	1502.6660	4.0000	1.0000	22731.9480
	1500	4.1099	0.3177	12.0070	3.5882	0.7365	2389.2140	4.0000	1.0000	44905.2730
B3	200	6.6826	0.7092	8.3850	6.0259	0.5457	4009.6040	6.9938	0.9449	19935.8860
	500	6.9143	0.9143	9.2810	6.3792	0.7040	3540.5920	6.9998	0.9986	45079.4920
	800	6.9670	0.9677	9.4190	6.5751	0.7859	2842.2780	7.0000	1.0000	64377.6220
	1500	6.9950	0.9950	15.3160	6.8065	0.8981	3476.0420	7.0000	1.0000	123651.9970
B4	200	8.9524	0.1073	11.2860	9.6522	0.3374	4611.1180	11.9939	0.9328	33431.1240
	500	8.9987	0.1136	13.2190	10.1836	0.4229	4454.6210	11.9996	0.9974	81908.7640
	800	9.0778	0.1245	16.3990	10.5306	0.4931	4685.9790	12.0000	1.0000	136090.3950
	1500	9.1444	0.1272	21.3990	11.0001	0.6095	4452.9270	12.0000	1.0000	225375.6450

(B2 and B4) is extremely poor, as we analyzed in Set. 3.3, mainly because $\phi_1 = \phi_2$ in these models.

In terms of calculation time (duration(s)), since the D-Ness algorithm finds the threshold value from closed-form expressions, it will be significantly faster than the other two methods, but the premise of using this algorithm is that T_{Wald-E} (3.6) rejects the null Hypothesis $H_0^{(1)}$. Otherwise, as in the previous analysis, it is impossible to find the true threshold value of the BiNB-MTTINAR(1) model. For $\hat{r}_{CLS}^{(2)}$, although its calculation speed is not as good as the D-Ness algorithm, it is faster than \hat{r}_{CML} , especially for a large sample size.

Based on the above analysis, we make the following recommendations. For a small sample size, our optimal choice for estimating the threshold value is \hat{r}_{CML} . For a large sample size, if we can test $\phi_1 \neq \phi_2$, the D-Ness algorithm is the optimal choice; otherwise, $\hat{r}_{CLS}^{(2)}$ is the best.

4.3 Size and Power of the Wald test

In this section, we will evaluate the performance of the test statistics T_{Wald-E} and $T_{Wald-Var}$. For the sake of readability, we introduce the following two INAR processes that are used in simulations:

$$INAR(1)\text{-Poisson: } X_t = \alpha_1 \circ X_{t-1} + Z_{1,t}, \quad (4.1)$$

$$INAR(1)\text{-Geo: } X_t = \alpha_2 * X_{t-1} + Z_{2,t}. \quad (4.2)$$

where “ $\alpha_1 \circ$ ”, “ $\alpha_2 *$ ”, $Z_{1,t}$, $Z_{2,t}$ are the same as in Definition 2.1.

For each simulation, the empirical sizes and empirical powers, the relative frequency of simulated sample paths leading to a rejection of the null (rejection rate), are calculated at the nominal level of 0.05 (the associated critical values are 3.8415 and 5.991). The repetition number is 10000, and the sample sizes $n = 200, 500, 800, 1000$ are used to calculate the empirical sizes and the sample sizes $n = 200, 500, 1000, 2000$ are used to calculate the empirical powers. We begin by calculating empirical sizes using observations produced by models (4.1) and (4.2), with the following parameter configurations taken into account:

Model(I-P₁): $(\alpha_1, \lambda) = (0.2, 6)$; Model(I-P₂): $(\alpha_1, \lambda) = (0.4, 5)$; Model(I-P₃): $(\alpha_1, \lambda) = (0.5, 5)$;

Model(I-G₁): $(\alpha_2, \lambda) = (0.4, 5)$; Model(I-G₂): $(\alpha_2, \lambda) = (0.5, 4)$; Model(I-G₃): $(\alpha_2, \lambda) = (0.6, 5)$;

Then, we calculate empirical powers using observations generated through the BiNB-MTTINAR(1) model (2.3) with the following parameter configurations:

Model(B-M₁): $(\phi_1, \phi_2, \lambda, r, R) = (0.4, 0.2, 6, 6, 0)$; Model(B-M₄): $(\phi_1, \phi_2, \lambda, r, R) = (0.4, 0.2, 6, 6, 1)$;

Model(B-M₂): $(\phi_1, \phi_2, \lambda, r, R) = (0.4, 0.4, 6, 6, 0)$; Model(B-M₅): $(\phi_1, \phi_2, \lambda, r, R) = (0.4, 0.4, 6, 6, 1)$;

Model(B-M₃): $(\phi_1, \phi_2, \lambda, r, R) = (0.3, 0.6, 5, 7, 0)$; Model(B-M₆): $(\phi_1, \phi_2, \lambda, r, R) = (0.3, 0.6, 5, 7, 1)$;

Among them, B-M₂ and B-M₄ models are the special cases in the BiNB-MTTINAR(1) model, with $\phi_1 = \phi_2$, and can be used to calculate the empirical sizes of T_{Wald-E} and the empirical powers of $T_{Wald-Var}$. Illustrative results concerning the size and power are shown in Tables 7 and 8.

As can be seen from Tables 7 and 8, both T_{Wald-E} and $T_{Wald-Var}$ achieve satisfactory performances, and the empirical sizes are closer to the significance level of 0.05 as the sample size increases. In particular, the empirical sizes of T_{Wald-E} approach the 0.05 level significantly faster, because the estimation of conditional variance can be regarded as the two-step CLS estimation based on $\hat{\theta}_{CLS}$, and its convergence rate must be slower than $\hat{\theta}_{CLS}$. For the Models B-M₂ and B-M₄, we expect that the true conclusion can be obtained through our tests: the existence of the segmented structure. However, as can be seen from Tables 7 and 8, T_{Wald-E} does not meet this expectation, which is consistent with our argument in Sect. 3.4.2 that T_{Wald-E} cannot be used to support the conclusion that the segmented structure does not exist. Based on the above analysis, we can draw the following conclusions. In practice, we can use T_{Wald-E} to test first, and if T_{Wald-E} rejects the null hypothesis, the piecewise structure exists. If T_{Wald-E} supports the null hypothesis, we need to check again using $T_{Wald-Var}$ to detect the existence of a piecewise structure.

Table 7: Empirical Sizes of T_{Wald-E} and $T_{Wald-Var}$ at level 0.05

Model	n	T_{Wald-E}	$T_{Wald-Var}$	Model	n	T_{Wald-E}	$T_{Wald-Var}$
I-P ₁	200	0.0293	0.0350	I-G ₁	200	0.0273	0.0425
	500	0.0345	0.0497		500	0.0525	0.0450
	800	0.0447	0.0548		800	0.0519	0.0494
	1000	0.0485	0.0522		1000	0.0490	0.0481
I-P ₂	200	0.0525	0.0048	I-G ₂	200	0.0523	0.0356
	500	0.0502	0.0250		500	0.0513	0.0490
	800	0.0484	0.0440		800	0.0505	0.0492
	1000	0.0483	0.0514		1000	0.0532	0.0506
I-P ₃	200	0.0543	0.0197	I-G ₃	200	0.0504	0.0337
	500	0.0561	0.0449		500	0.0521	0.0527
	800	0.0526	0.0577		800	0.0506	0.0549
	1000	0.0503	0.0521		1000	0.0526	0.0568
B-M ₂	200	0.0287		B-M ₅	200	0.0242	
	500	0.0490			500	0.0562	
	800	0.0501			800	0.0556	
	1000	0.0504			1000	0.0542	

Table 8: Empirical Power of T_{Wald-E} and $T_{Wald-Var}$ at level 0.05

Model	n	T_{Wald-E}	$T_{Wald-Var}$	Model	n	T_{Wald-E}	$T_{Wald-Var}$
B-M ₁	200	0.2889	0.3448	B-M ₄	200	0.0585	0.0807
	500	0.5284	0.6524		500	0.2364	0.2415
	1000	0.8171	0.8396		1000	0.3988	0.5538
	2000	0.9778	0.9512		2000	0.6301	0.8963
B-M ₂	200		0.3904	B-M ₅	200		0.0501
	500		0.7228		500		0.1274
	1000		0.9148		1000		0.3216
	2000		0.9836		2000		0.6976
B-M ₃	200	0.5983	0.2373	B-M ₆	200	0.4881	0.1085
	500	0.9204	0.5676		500	0.8759	0.3782
	1000	0.9971	0.8762		1000	0.9948	0.7810
	2000	1.0000	0.9856		2000	1.0000	0.9821

5 Real Data Example

In this section, we discuss possible applications of the introduced BiNB-MTTINAR(1) model. We consider the datasets from The Forecasting Principles site (<http://www.forecastingprinciples.com>), in the section about Crime - Pittsburgh police car beat data. The data set recorded the number of monthly occurrences of 36 types of crime in 66 police departments in Pittsburgh, and has been partially analyzed by [Zhu \(2012\)](#), [Zhang et al. \(2020\)](#) and [Zhang et al. \(2022\)](#), among others. For this example, we focus on the counts of criminal mischief in the 14th police car beat in Pittsburgh. The data consist of 144 observations, starting in January 1990 and ending in December 2001.

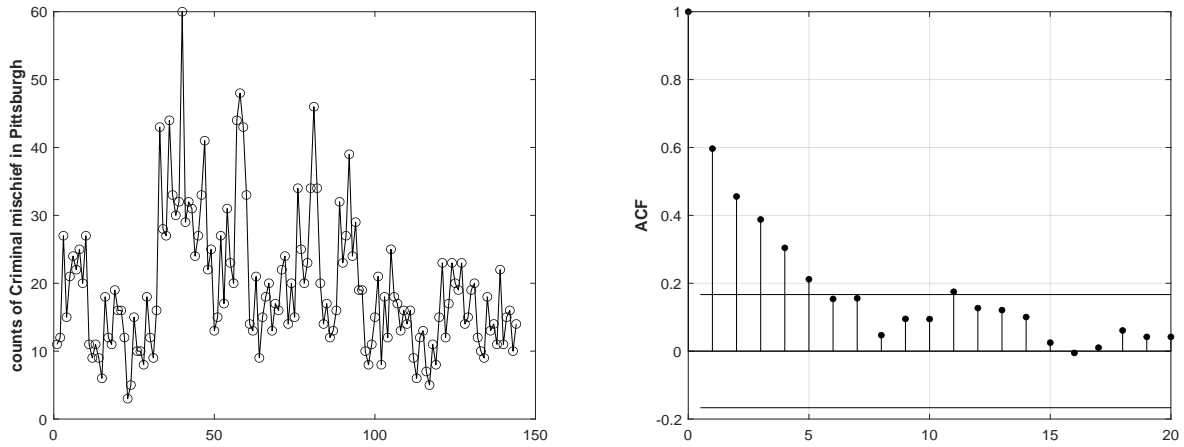


Fig. 4 Sample path and ACF of the monthly counts of Criminal mischief in Pittsburgh (from January 1990 and ending in December 2001).

Figure 4 shows the sample path and the sample autocorrelation (ACF) of the observations. We start with fitting the BiNB-MTTINAR(1) (when $R = 0$) model to the data (later, we also consider the more general SETINAR models). We estimate the model parameters for threshold values of $r \in \{9, \dots, 33\}$, where 9 and 33 are the 10th and 90th quantiles of the data. After minimizing (3.3), we decide to consider a model with a threshold value $\hat{r}_{CML} = 11$. Then, we applied the Wald test (3.6) to check whether such a nonlinear model is appropriate for the data. We obtain $T_{Wald-E} = 3.9636$, while our critical value on a 0.05 level is 3.8415, so we have to reject the null hypothesis $\phi_1 = \phi_2$. It should be noted that if the T_{Wald-E} obtained is less than 3.8415, we need to further apply $T_{Wald-Var}$ (3.8) to check for the existence of a piecewise structure.

Next, we use the BiNB-MTTINAR(1) model and the following integer-valued threshold autoregressive models to fit the criminal mischief incident dataset and compare different models via the AIC and BIC.

- SETINAR(2,1) model ([Monteiro et al. \(2012\)](#)).
- NBTINAR(1) model ([Yang et al. \(2018\)](#)).
- RCTINAR(1) model ([Li et al. \(2018\)](#)).

For each of the above models, the CML of the parameters and the threshold r , the standard error (SE) of $\hat{\theta}_{CML}$, the root mean square of differences between observations and forecasts (RMS), and the AIC and BIC values are given. Among them, the standard error for the CML estimator can be obtained as the square roots of the elements in the diagonal of the inverse of the negative Hessian of the log-likelihood calculated at the CML estimates. RMS is defined as follows

$$\text{RMS} = \sqrt{\frac{1}{n-1} \sum_{t=2}^n (X_t - \hat{\phi}_1 X_{t-1} I_{1,t}^R - \hat{\phi}_2 X_{t-1} I_{2,t}^R - \hat{\lambda})^2}$$

The fitting results are summarized in Table 9. As seen from the results presented in Table 9, the parameter α_1 estimators for the SETINAR(2,1) and NBTINAR(1) models are poor since they are close to the boundaries 0 and 1 and are not significant regarding the approximated standard errors. Therefore, these two models are not suitable for fitting this dataset. Furthermore, when comparing the SETINAR(2,1) and RCTINAR(1) models, we find that all of their parameter estimations are similar. The outcome of RCTINAR(1) is very superior to that of SETINAR when taking AIC and BIC into account as information criteria. This conclusion is consistent with the finding in Li et al. (2018), which states that SETINAR(2,1) is a special case of the RCTINAR(1) model.

Then, we compute the (standardized) Pearson residuals, $\text{Pr}_t(\hat{\theta})$ (Weiß et al. , 2019), to check if the fitted model is adequate for the data.

$$\text{Pr}_t(\hat{\theta}) = \frac{X_t - \hat{\phi}_1 X_{t-1} I_{1,t}^R - \hat{\phi}_2 X_{t-1} I_{2,t}^R - \hat{\lambda}}{\sqrt{(\hat{\phi}_1(1 - \hat{\phi}_1)X_{t-1} + \hat{\lambda})I_{1,t}^R + (\hat{\phi}_2(1 + \hat{\phi}_2)X_{t-1} + \hat{\lambda}(1 + \hat{\lambda}))I_{2,t}^R}}. \quad (5.1)$$

After computing, the mean and the variance of $\text{Pr}_t(\hat{\theta})$ are -0.0483 and 1.0653 , which are close to 0 and 1, indicating that the fitted model is adequate. Furthermore, Figure 5 shows the diagnostic checking plots for our out fitted model, including (a) Standardized residuals, (b) Histogram of standardized residuals, (c) ACF plot of residuals, and (d) PACF plot of residuals. As can be roughly seen from the residuals sample plot (Figure 5(a)), the estimated residuals indicate that the series is stationary, and the Pearson residuals samples ACF and PACF have values close to zero, which reveals that our fitted model is suitable.

Finally, all estimators of the BiNB-MTINAR(1) ($R = 0$) model are significant regarding the approximated standard errors, and the BiNB-MTINAR(1) ($R = 0$) model has the lowest RMS, AIC, and BIC of all models and is the model of choice considering these information criteria.

A useful and significant problem in time series analysis is the prediction problem. Under the standard framework, conditional expectation is the frequently used approach for constructing predictors since it can yield predictors with the optimal property in terms of the mean squared error. However, the conditional expectation method violates data coherence since it can hardly produce integer-valued predictors. Therefore, we want an appropriate method that can generate predictors with integer values. Freeland and McCabe (2004) proposed a workable method that uses the h -step-ahead conditional distribution to forecast the future value. One can obtain the point predictor from the median or the mode of the h -step-ahead conditional

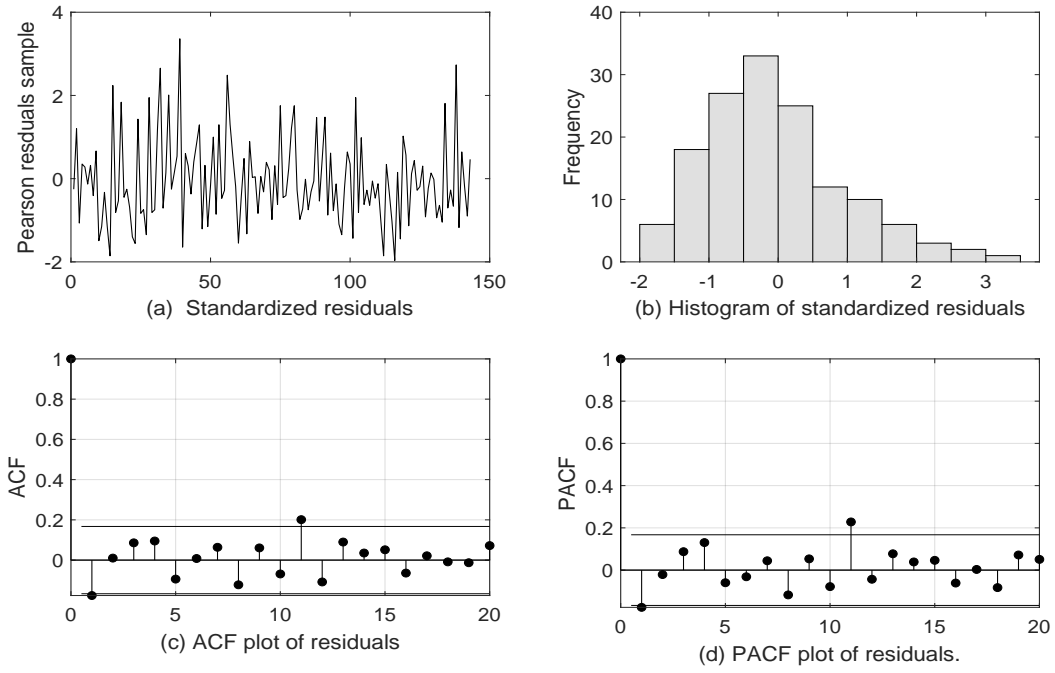


Fig. 5 Diagnostic checking plots for the Criminal mischief in Pittsburgh data.

Table 9: Fitting results of different models: CML, \hat{r}_{CML} , SE, RMS, AIC and BIC

Model	Para.	CML	SE	\hat{r}_{CML}	RMS	AIC	BIC
SETINAR(2,1)	α_1	0.0000	3.5494	14	8.0297	1140.5533	1149.4627
	α_2	0.3454	0.0048				
	λ	14.0482	0.0010				
NBTINAR(1)	α_1	1.0000	0.6167	17	7.9392	984.8061	993.7155
	α_2	0.7811	0.0061				
	v	3.0000	0.0014				
RCTINAR(1)	ϕ_1	0.0744	0.0054	14	7.9888	1009.0917	1018.0011
	ϕ_2	0.3751	0.0029				
	λ	13.2755	0.0004				
BiNB-MTTINAR(1) (R=0)	ϕ_1	0.3872	0.0029	11	7.9261	974.2542	983.1636
	ϕ_2	0.6098	0.0029				
	λ	8.5907	0.0005				
BiNB-MTTINAR(1) (R=1)	ϕ_1	0.5508	0.0006	33	8.0711	998.5767	1007.4862
	ϕ_2	0.6581	0.0010				
	λ	7.6882	0.0012				

distribution. This method has been employed by some researchers, see [Maiti and Biswas \(2017\)](#), [Li et al. \(2018\)](#), [Kang et al. \(2021\)](#). Learning from this idea, it is possible to calculate the h -step-ahead conditional distribution for the BiNB-MTINAR(1) model by taking powers of the transition matrix since we are interested in a Markov chain. To be more precise, one may calculate the h -step-ahead conditional distribution of X_{t+h} given X_t by

$$P(X_{t+h} = j | X_t = i) = [\mathbf{P}^h]_{i+1, j+1},$$

where \mathbf{P} denotes the transition matrix defined by the following equation,

$$\mathbf{P} = (P_{ij})_{i,j=0,1,2,\dots}, \quad (5.2)$$

and $P_{ij} = P(X_t = j | X_{t-1} = i)$ is the transition probability, which is given in Equation (2.4). For illustration purposes, we compute the mean and mode of the h -step-ahead conditional distribution for the BiNB-MTINAR(1) ($R = 0$) model and their corresponding bias and the mean absolute deviation error (MADE) are considered in Table 10, where MADE is defined as follows:

$$\text{MADE} = \frac{1}{n-1} \sum_{t=1}^n |\hat{X}_t - X_t|.$$

From the result in Table 10, the bias and MADE of the proposed predictors are acceptable. Therefore, based on the above analysis, we can conclude that the BiNB-MTINAR(1) (when $R = 0$) model is appropriate for this data set.

Table 10: Bias and MADE for h -step ahead predictions of the crime data: Criminal mischief

h	Expectation		Mode	
	Bias	MADE	Bias	MADE
1	-1.5378	1.5378	-2.0000	2.0000
5	1.8176	2.4252	1.6000	2.4000
10	-0.6992	2.7403	-1.0000	2.8000
20	-0.9485	3.1871	-1.0500	3.2500
30	-0.6581	3.9260	-0.7667	3.8333

6 Conclusions

This article introduced a new first-order mixture integer-valued threshold autoregressive process based on the binomial and negative binomial thinning operators. The process is proven to be stationary and ergodic. We investigated the CLS and the CML techniques for parameter estimation, and the estimators' asymptotic properties are demonstrated. Two methods are suggested for estimating the unknown threshold parameter r , based on the CLS and CML score functions. Additionally, to check for the existence of piecewise

structure, we constructed two types Wald test statistics for conditional expectation and conditional variance parameters, respectively. We successfully applied the BiNB-MTINAR(1) model to crime time series dataset. Potential issues for future research include extending the results to multivariate cases and considering mixture threshold INAR models based on generalized thinning operator. These remain topics for future study.

Acknowledgements

The authors thank the Joint Editor, Associate Editor and two reviewers for helpful comments, which led to a much improved version of the paper. This work is supported by National Natural Science Foundation of China (No.12171463, 11871028, 11731015, 12001229, 11901053, 12001229).

Appendix

Proof of Proposition 2.1 Considering that the case $R = 0$ is similar to $R = 1$, we only prove the case $R = 0$. It is easy to see that $\{X_t\}_{t \in \mathbb{Z}}$ is a Markov chain with state space \mathbb{N}_0 . From the expression of transition probabilities defined in (2.4), it follows that the chain is irreducible and aperiodic. Furthermore, to show that $\{X_t\}_{t \in \mathbb{Z}}$ is positive recurrent it is sufficient to prove that $\sum_{t=1}^{\infty} P^t(0, 0) = +\infty$ (since $\{X_t\}_{t \in \mathbb{Z}}$ is irreducible) with $P^t(x, y) := P(X_t = y | X_0 = x)$. For convenience we denote

$$S_t = \begin{cases} 0, & \text{if } X_{t-1} \leq r, \\ 1, & \text{if } X_{t-1} > r. \end{cases} \quad \otimes_t := \begin{cases} \circ, & \text{if } X_{t-1} \leq r, \\ *, & \text{if } X_{t-1} > r. \end{cases} \quad U_i = \begin{cases} e^{-\lambda}, & i = 1, \\ \frac{1}{1+\lambda}, & i = 2. \end{cases}$$

Then (2.3) can be rewritten as

$$X_t = \phi_{S_t+1} \otimes_t X_{t-1} + Z_{S_t+1,t}. \quad (1)$$

By iterating (1) $t - 1$ times, we have

$$X_t = \phi_{S_t+1} \otimes_t \phi_{S_{t-1}+1} \otimes_{t-1} \cdots \otimes_2 \phi_{S_1+1} \otimes_1 X_0 + \left(\sum_{i=1}^{t-1} \phi_{S_t+1} \otimes_t \phi_{S_{t-1}+1} \otimes_{t-1} \cdots \otimes_{i+2} \phi_{S_{i+1}+1} \otimes_{i+1} Z_{S_i+1,i} \right) + Z_{S_t+1,t}.$$

This allows us to write

$$\begin{aligned} P^t(0, 0) &= P\left(\left(\sum_{i=1}^{t-1} \phi_{S_t+1} \otimes_t \phi_{S_{t-1}+1} \otimes_{t-1} \cdots \otimes_{i+2} \phi_{S_{i+1}+1} \otimes_{i+1} Z_{S_i+1,i}\right) + Z_{S_t+1,t} = 0 \mid X_0 = 0\right) \\ &= P(Z_{S_t+1,t} = 0, \phi_{S_t+1} \otimes_t Z_{S_{t-1}+1,t-1} = 0, \cdots, \phi_{S_t+1} \otimes_t \cdots \otimes_3 \phi_{S_2+1} \otimes_2 Z_{S_1+1,1} = 0 \mid X_0 = 0) \\ &= \sum_{i_1=1}^2 \sum_{i_2=1}^2 \cdots \sum_{i_t=1}^2 P(S_1 + 1 = i_1, S_2 + 1 = i_2, \cdots, S_t + 1 = i_t \mid X_0 = 0) \\ &\quad \times P(Z_{S_t+1,t} = 0, \phi_{i_t} \otimes_t Z_{i_{t-1}+1,t-1} = 0, \cdots, \phi_{i_t} \otimes_t \cdots \otimes_3 \phi_{i_2} \otimes_2 Z_{i_1+1,1} = 0 \mid X_0 = 0) \end{aligned}$$

By the definition of the binomial thinning operator “ \circ ” and the negative binomial thinning operator “ $*$ ”, we have

$$P(\phi_i \otimes X = 0) = \begin{cases} P(\phi_1 \circ X = 0) = \sum_{m=0}^{+\infty} (1 - \phi_1)^m P(X = m), & \text{if } i = 1, \\ P(\phi_2 * X = 0) = \sum_{m=0}^{+\infty} (1 + \phi_2)^{-m} P(X = m), & \text{if } i = 2. \end{cases} \quad (2)$$

Obviously, if X is not always equal to 0, $P(\phi_i \otimes X = 0) > P(X = 0)$, $i = 1, 2$. Let k denote the number of the sequence $\{X_t \leq r\}_{t \in \mathbb{Z}}$. By (2) we have

$$\begin{aligned} P^t(0, 0) &> \sum_{i_1=1}^2 \sum_{i_2=1}^2 \cdots \sum_{i_t=1}^2 P(S_1 + 1 = i_1, S_2 + 1 = i_2, \dots, S_t + 1 = i_t | X_0 = 0) \\ &\quad \times U_{i_t} U_{i_{t-1}} \cdots U_{i_1} \\ &= \sum_{i_1=1}^2 \sum_{i_2=1}^2 \cdots \sum_{i_t=1}^2 P(S_1 + 1 = i_1, S_2 + 1 = i_2, \dots, S_t + 1 = i_t | X_0 = 0) \\ &\quad \times e^{-k\lambda} \left(\frac{1}{1+\lambda} \right)^{t-k} \end{aligned}$$

Since $\lim_{t \rightarrow \infty} e^{-k\lambda} \left(\frac{1}{1+\lambda} \right)^{t-k} = 0$, which implies that $\lim_{t \rightarrow \infty} P^t(0, 0) \neq 0$. Therefore, we conclude that $\sum_{t=1}^{\infty} P^t(0, 0) = +\infty$. This proves that $\{X_t\}$ is a positive recurrent Markov chain (and hence ergodic) which ensures the existence of a strictly stationary distribution of BiNB-MTTINAR(1) process.

Proof of Proposition 2.2 To show this, we denote $\phi_{\max} = \max\{\phi_1, \phi_2\}$. Compute to see that, under the stationary distribution,

$$\begin{aligned} E(X_t) &= E[(\phi_1 \circ X_{t-1})I_{1,t}^R] + E[(\phi_2 * X_{t-1})I_{2,t}^R] + \lambda \\ &= E[E((\phi_1 \circ X_{t-1})I_{1,t}^R | X_{t-1})] + E[E((\phi_2 * X_{t-1})I_{2,t}^R | X_{t-1})] + \lambda \\ &\leq \phi_{\max} E(X_{t-1}) + \lambda \\ &\leq \cdots \\ &\leq (\phi_{\max})^t E(X_0) + \lambda \sum_{i=0}^{t-1} (\phi_{\max})^i \leq \infty, \end{aligned} \tag{3}$$

where $\phi_{\max} = \max\{\phi_1, \phi_2\}$.

Similarly, we have

$$\begin{aligned} E(X_t^2) &= [E(\phi_1 \circ X_{t-1})^2 + 2E(\phi_1 \circ X_{t-1})E(Z_{1,t}) + E(Z_{1,t})^2] I_{1,t}^R \\ &\quad + [E(\phi_2 * X_{t-1})^2 + 2E(\phi_2 * X_{t-1})E(Z_{2,t}) + E(Z_{2,t})^2] I_{2,t}^R \\ &= [(\phi_1 - \phi_1^2 + 2\phi_1\lambda)E(X_{t-1}) + \phi_1^2 E(X_{t-1}^2) + \lambda + \lambda^2] I_{1,t}^R \\ &\quad + [(\phi_2 + \phi_2^2 + 2\phi_2\lambda)E(X_{t-1}) + \phi_2^2 E(X_{t-1}^2) + \lambda + 2\lambda^2] I_{2,t}^R \\ &\leq u_{\max} E(X_{t-1}) + \phi_{\max}^2 E(X_{t-1}^2) + \lambda + 2\lambda^2 \end{aligned}$$

where $u_{\max} = \max\{(\phi_1 - \phi_1^2 + 2\phi_1\lambda), (\phi_2 + \phi_2^2 + 2\phi_2\lambda)\}$.

If $t = 1$, $E(X_1^2) \leq u_{\max} E(X_0) + \phi_{\max}^2 E(X_0^2) + \lambda + 2\lambda^2 < \infty$.

Else if $t \geq 2$,

$$\begin{aligned} E(X_t^2) &\leq \sum_{i=0}^{t-1} u_{\max} \phi_{\max}^{t-1+i} E(X_0) + \lambda \sum_{i=0}^{t-2} u_{\max} \phi_{\max}^{t-2+i} + (\lambda + 2\lambda^2) \sum_{i=0}^{t-1} \phi_{\max}^{2i} \\ &< \infty. \end{aligned} \tag{4}$$

Some similar but tedious calculation shows that $E(X_t^3) \leq \infty$. Combining (3) and (4), one can see that $E(X_t^k) < \infty$ for $k = 1, 2, 3$. \square

Proof of Proposition 2.3 The results (i) to (iii) are straightforward to verify. We give the proof of (iv) only.

(iv) The variance of X_t is given by

$$\begin{aligned} \text{Var}(X_t) &= \text{Var}[I_{1,t}^R(\phi_1 \circ X_{t-1} + Z_{1,t})] + \text{Var}[I_{2,t}^R(\phi_2 * X_{t-1} + Z_{2,t})] \\ &\quad + 2\text{Cov}(I_{1,t}^R(\phi_1 \circ X_{t-1} + Z_{1,t}), I_{2,t}^R(\phi_2 * X_{t-1} + Z_{2,t})) \\ &= I + II + III. \end{aligned} \tag{5}$$

A direct calculation shows

$$\begin{aligned} I &= \text{Var} [E(I_{1,t}^R(\phi_1 \circ X_{t-1} + Z_{1,t})|X_{t-1})] + E [\text{Var}(I_{1,t}^R(\phi_1 \circ X_{t-1} + Z_{1,t})|X_{t-1})] \\ &= \phi_1^2 \text{Var}(I_{1,t}^R X_{t-1}) + q\lambda + E(I_{1,t}^R(\phi_1(1 - \phi_1)X_{t-1})) \\ &= \phi_1^2 \text{Var}(I_{1,t}^R X_{t-1}) + q\lambda + q\phi_1(1 - \phi_1)\mu_1 \\ &= \phi_1^2 E(I_{1,t}^R X_{t-1}^2) - \phi_1^2 q^2 \mu_1^2 + q\lambda + q\phi_1(1 - \phi_1)\mu_1 \\ &= q(\phi_1^2 \sigma_1^2 + \phi_1(1 - \phi_1)\mu_1) + q(1 - q)\phi_1^2 \mu_1^2 + q\lambda \end{aligned} \tag{6}$$

Similarly, we have

$$\begin{aligned} II &= \text{Var} [E(I_{2,t}^R(\phi_2 * X_{t-1} + Z_{2,t})|X_{t-1})] + E [\text{Var}(I_{2,t}^R(\phi_2 * X_{t-1} + Z_{2,t})|X_{t-1})] \\ &= \phi_2^2 \text{Var}(I_{2,t}^R X_{t-1}) + (1 - q)\lambda(1 + \lambda) + E(I_{2,t}^R(\phi_2(1 + \phi_2)X_{t-1})) \\ &= \phi_2^2 E(I_{2,t}^R X_{t-1}^2) - \phi_2^2(1 - q)^2 \mu_2^2 + (1 - q)\lambda(1 + \lambda) + (1 - q)\phi_2(1 + \phi_2)\mu_2 \\ &= (1 - q)(\phi_2^2 \sigma_2^2 + \phi_2(1 + \phi_2)\mu_2) + q(1 - q)\phi_2^2 \mu_2^2 + (1 - q)\lambda(1 + \lambda) \end{aligned} \tag{7}$$

and

$$\begin{aligned} III &= 2\text{Cov}(I_{1,t}^R(\phi_1 \circ X_{t-1} + Z_{1,t}), I_{2,t}^R(\phi_2 * X_{t-1} + Z_{2,t})) \\ &= -2q(1 - q)(\phi_1 \mu_1 + \lambda)(\phi_2 \mu_2 + \lambda). \end{aligned} \tag{8}$$

Then, (iv) follows by replacing (6), (7) and (8) in (5) and some algebra.

(v): For the autocovariance $\text{Cov}(X_t, X_{t+h})$, when $h = 1$,

$$\begin{aligned} \text{Cov}(X_t, X_{t+1}) &= \text{Cov}[X_t, E(X_{t+1}|X_t)] \\ &= \text{Cov}\{X_t, [\phi_1 X_t + \lambda]I_{1,t+1}^R + [\phi_2 X_t + \lambda]I_{2,t+1}^R\} \\ &= \sum_{s=1}^2 [\phi_s \text{Cov}(X_t, I_{s,t+1}^R X_t)], \end{aligned}$$

where

$$\text{Cov}(X_t, I_{s,t+1}^R X_t) = E(I_{s,t+1}^R X_t X_t) - E(I_{s,t+1}^R X_t)E(X_t) = p_s(\sigma_s^2 + \mu_s^2) - p_s \mu_s E(X_t),$$

Then,

$$\text{Cov}(X_t, X_{t+1}) = \sum_{s=1}^2 \{ \phi_s p_s [(\sigma_s^2 + \mu_s^2) - \mu_s \mathbb{E}(X_t)] \} = \sum_{s=1}^2 \phi_s p_s \gamma_0^{(s)},$$

when $h > 1$, there is

$$\begin{aligned} \text{Cov}(X_t, X_{t+h}) &= \text{Cov}[X_t, \mathbb{E}(X_{t+h} | X_{t+h-1})] \\ &= \text{Cov}\{X_t, (\phi_1 X_{t+h-1} + \lambda) I_{1,t+h}^R + (\phi_2 X_{t+h-1} + \lambda) I_{2,t+h}^R\} \\ &= \sum_{s=1}^2 \phi_s [\text{Cov}(X_t, I_{s,t+h}^R X_{t+h-1})], \end{aligned}$$

where

$$\text{Cov}(X_t, I_{s,t+h}^R X_{t+h-1}) = p_s \text{Cov}(X_t, X_{t+h-1} | X_{t+h-1} \leq r) = p_s \gamma_{h-1}^{(s)},$$

Then, we obtain

$$\text{Cov}(X_t, X_{t+h}) = \sum_{s=1}^2 \phi_s p_s \gamma_{h-1}^{(s)}.$$

Thus, the autocorrelation function $\rho(h) = [\sum_{s=1}^2 \phi_s p_s \gamma_{h-1}^{(s)}] \setminus \text{Var}(X_t)$. \square

Proof of Theorems 3.2 We first prove the consistency of $\hat{\theta}_{CML}$. Let Θ be the parametric space: $(0, 1)^2 \times (0, +\infty)$. From (2.4), $\ell(\theta)$ is a measurable function of X_t for all $\theta \in \Theta$, and $\partial \ell(\theta) / \partial \theta$ exists and is continuous in an open neighborhood $N_1(\theta_0)$ of θ_0 . Therefore, in order to prove the existence and consistency of the CML estimators, it is sufficient to show that assumption (c) of Theorems 4.1.2 in Amemiya (1985) holds. Note that $\ell_t(\theta)$ is continuous in an open and convex neighborhood $N_2(\theta_0)$, thus there at least exists a point $\theta_1 \in N_2(\theta_0)$ such that $\ell_t(\theta)$ attains the maximum value at θ_1 , i.e.,

$$\mathbb{E} \left(\sup_{\theta \in N_2(\theta_0)} \ell_t(\theta) \right) = \mathbb{E} [\log P(X_t | \mathcal{F}_{t-1})]_{\theta_1} \leq \log [\mathbb{E} (P(X_t | \mathcal{F}_{t-1}))]_{\theta_1} < \infty. \quad (9)$$

From Proposition 2.1, $\{X_t\}$ is stationary and ergodic, it follows $\frac{1}{n} \sum_{t=1}^n \ell_t(\theta) \rightarrow \mathbb{E} \ell_t(\theta)$ in probability as $n \rightarrow \infty$. By Jensen's inequality, we have

$$\mathbb{E}(\ell_t(\theta) - \ell_t(\theta_0)) = \mathbb{E} \left[\log \frac{P(X_t | \mathcal{F}_{t-1})_{\theta}}{P(X_t | \mathcal{F}_{t-1})_{\theta_0}} \right] \leq \log \left[\mathbb{E} \frac{P(X_t | \mathcal{F}_{t-1})_{\theta}}{P(X_t | \mathcal{F}_{t-1})_{\theta_0}} \right] = 0. \quad (10)$$

From (9) and (10), $\mathbb{E}(\ell_t(\theta))$ is a strict local maximum at θ_0 . Hence, the assumption (c) is true, the proof of consistency is complete.

To prove asymptotically, we perform Taylor expansion of the score vector around θ_0 .

$$\mathbf{0} = \frac{1}{\sqrt{n}} \frac{\partial \ell(\hat{\theta}_{CML})}{\partial \theta} = \frac{1}{\sqrt{n}} \frac{\partial \ell(\theta_0)}{\partial \theta} + \left(\frac{1}{n} \frac{\partial^2 \ell(\theta^*)}{\partial \theta \partial \theta^T} \right) \sqrt{n}(\hat{\theta}_{CML} - \theta_0), \quad (11)$$

where θ^* lies in between $\hat{\theta}_{CML}$ and θ_0 . According to Theorem 4.1.3 in Amemiya (1985), we divide the proof into the following four steps.

Step 1: It is easy to see $E \frac{\partial l_t(\boldsymbol{\theta}_0)}{\partial \boldsymbol{\theta}} = \mathbf{0}$, thus $Cov \left(\frac{\partial l_t(\boldsymbol{\theta}_0)}{\partial \boldsymbol{\theta}} \right) = E \left[\left(\frac{\partial l_t(\boldsymbol{\theta}_0)}{\partial \boldsymbol{\theta}} \right) \left(\frac{\partial l_t(\boldsymbol{\theta}_0)}{\partial \boldsymbol{\theta}} \right)^T \right]$. Using the ergodic theorem,

$$\frac{1}{n} \frac{\partial l(\boldsymbol{\theta}_0)}{\partial \boldsymbol{\theta}} \rightarrow E \left(\frac{1}{P(X_t|\mathcal{F}_{t-1})} \frac{\partial P(X_t|\mathcal{F}_{t-1})}{\partial \boldsymbol{\theta}} \right)_{\boldsymbol{\theta}_0} \text{ in probability one.}$$

Using the martingale central limit theorem and the Cramér-Wold device, We can get that

$$\frac{1}{\sqrt{n}} \frac{\partial l(\boldsymbol{\theta}_0)}{\partial \boldsymbol{\theta}} \xrightarrow{d} N(\mathbf{0}, \mathbf{I}(\boldsymbol{\theta}_0)), \quad (12)$$

where $\mathbf{I}(\boldsymbol{\theta}_0) = E \left[\frac{\partial l_t(\boldsymbol{\theta})}{\partial \boldsymbol{\theta}} \frac{\partial l_t(\boldsymbol{\theta})}{\partial \boldsymbol{\theta}^T} \right]_{\boldsymbol{\theta}_0}$.

Step 2: From (2.5), all the partial derivatives $\frac{\partial l(\boldsymbol{\theta})}{\partial \theta_i}$ exist and three times continuous differentiable in $\boldsymbol{\Theta}$, thus $\frac{\partial^2 l(\boldsymbol{\theta})}{\partial \theta_i \partial \theta_j}$ exists and is continuous in an open, convex neighborhood of $\boldsymbol{\theta}_0$ ($\boldsymbol{\theta}_2 \in N(\boldsymbol{\theta}_0)$).

Step 3: From Step 2, there at least exists a point $\boldsymbol{\theta}_2 \in N(\boldsymbol{\theta}_0)$ such that $\frac{\partial^2 l(\boldsymbol{\theta})}{\partial \theta_i \partial \theta_j}$ attains the maximum value at $\boldsymbol{\theta}_2$, i.e.,

$$E \left[\sup_{\boldsymbol{\theta} \in N(\boldsymbol{\theta}_0)} \left(\frac{\partial^2 l(\boldsymbol{\theta})}{\partial \theta_i \partial \theta_j} \right) \right] = E \left(\frac{\partial^2 l(\boldsymbol{\theta})}{\partial \theta_i \partial \theta_j} \right)_{\boldsymbol{\theta}_2} < \infty.$$

For convenience, we denote $\frac{\partial^2 l(\boldsymbol{\theta})}{\partial \boldsymbol{\theta} \partial \boldsymbol{\theta}^T} = H(X_t, \boldsymbol{\theta}) = (h_{ij}(X_t, \boldsymbol{\theta}))$ and $E \frac{\partial^2 l(\boldsymbol{\theta})}{\partial \boldsymbol{\theta} \partial \boldsymbol{\theta}^T} = H(\boldsymbol{\theta}) = (h_{ij}(\boldsymbol{\theta}))$. We only need to prove $h_{ij}(X_t, \boldsymbol{\theta})$ converges to a finite and non-stochastic function $h_{ij}(\boldsymbol{\theta}) = E(h_{ij}(X_t, \boldsymbol{\theta}))$. For $E(h_{ij}(\boldsymbol{\theta}) - E(h_{ij}(X_t, \boldsymbol{\theta}))) = 0$, i.e.,

$$\sup_{\boldsymbol{\theta} \in \boldsymbol{\Theta}} \left\| \frac{1}{n} \sum_{t=1}^n \frac{\partial^2 l_t(\boldsymbol{\theta}^0)}{\partial \boldsymbol{\theta} \partial \boldsymbol{\theta}^T} - E \frac{\partial^2 l(\boldsymbol{\theta}^0)}{\partial \boldsymbol{\theta} \partial \boldsymbol{\theta}^T} \right\| = o_p(1).$$

where $o_p(1)$ denote a random sequence converging to 0 in probability.

Step 4: We check that $\mathbf{J}(\boldsymbol{\theta}_0) = E \left[\frac{\partial^2 l_t(\boldsymbol{\theta})}{\partial \boldsymbol{\theta} \partial \boldsymbol{\theta}^T} \right]_{\boldsymbol{\theta}_0}$ is nonsingular. From the transition probability (2.4), after some algebra, we have $E \left(\frac{\partial^2}{\partial \theta_i^2} \log P(x_{t-1}, x_t) \right) < \infty$, $i = 1, 2, 3$ and $\frac{\partial^2}{\partial \phi_1 \partial \phi_2} \log P(x_{t-1}, x_t) = \frac{\partial^2}{\partial \phi_2 \partial \phi_1} \log P(x_{t-1}, x_t) = 0$, so we just need to prove that the following condition is true,

$$E \left(\frac{\partial^2}{\partial \lambda \partial \phi_i} \log P(x_{t-1}, x_t) \right) = E \left(\frac{\partial^2}{\partial \phi_i \partial \lambda} \log P(x_{t-1}, x_t) \right) < \infty, \quad i = 1, 2.$$

For convenience, we denote

$$\begin{aligned} p_1(x_{t-1}, x_t, \phi_1, \lambda) &= \sum_{m=0}^{\min(x_{t-1}, x_t)} \binom{i}{m} e^{-\lambda} \frac{\lambda^{j-m}}{(j-m)!} \phi_1^m (1-\phi_1)^{i-m} \\ &= \sum_{m=0}^{\min(x_{t-1}, x_t)} \rho_1(m, x_{t-1}, x_t, \phi_1, \lambda) \\ p_2(x_{t-1}, x_t, \phi_2, \lambda) &= \sum_{m=0}^{x_t} \frac{\Gamma(i+m)}{\Gamma(i)\Gamma(m+1)} \frac{\phi_2^m}{(1+\phi_2)^{i+m}} \frac{\lambda^{j-m}}{(1+\lambda)^{j-m+1}} \\ &= \sum_{m=0}^{x_t} \rho_2(m, x_{t-1}, x_t, \phi_2, \lambda), \end{aligned}$$

we conclude that,

$$\begin{aligned}\frac{\partial \rho_1(m, x_{t-1}, x_t, \phi_1, \lambda)}{\partial \phi_1} &= \left(\frac{m}{\phi_1} - \frac{x_{t-1} - m}{1 - \phi_1}\right) \rho_1(m, x_{t-1}, x_t, \phi_1, \lambda), \\ \frac{\partial \rho_2(m, x_{t-1}, x_t, \phi_2, \lambda)}{\partial \phi_2} &= \left(\frac{m}{\phi_2} + \frac{x_{t-1} + m}{1 + \phi_2}\right) \rho_2(m, x_{t-1}, x_t, \phi_2, \lambda), \\ \frac{\partial \rho_1(m, x_{t-1}, x_t, \phi_1, \lambda)}{\partial \lambda} &= \left(\frac{x_t - m}{\lambda} - 1\right) \rho_1(m, x_{t-1}, x_t, \phi_1, \lambda), \\ \frac{\partial \rho_2(m, x_{t-1}, x_t, \phi_2, \lambda)}{\partial \lambda} &= \left(\frac{x_t - m}{\lambda} - \frac{x_t - m + 1}{1 + \lambda}\right) \rho_2(m, x_{t-1}, x_t, \phi_2, \lambda).\end{aligned}$$

For $\frac{\partial^2}{\partial \phi_1 \partial \lambda} \log P(x_{t-1}, x_t)$,

$$\begin{aligned}\frac{\partial^2}{\partial \phi_1 \partial \lambda} \log P(x_{t-1}, x_t) &= \frac{\partial^2}{\partial \lambda \partial \phi_1} \log P(x_{t-1}, x_t) = -\frac{1}{(P(x_{t-1}, x_t))^2} \\ &\times \left[\left(\sum_{m=0}^{x_t} \left(\frac{x_t - m}{\lambda} - 1 \right) \rho_1(m, x_{t-1}, x_t, \phi_1, \lambda) \right) \left(\sum_{m=0}^{x_t} \left(\frac{m}{\phi_1} - \frac{x_{t-1} - m}{1 - \phi_1} \right) \rho_1(m, x_{t-1}, x_t, \phi_1, \lambda) \right) \right] I_{1,t}^R \\ &+ \frac{1}{P(x_{t-1}, x_t)} \left(\sum_{m=0}^{x_t} \left(\frac{x_t - m}{\lambda} - 1 \right) \left(\frac{m}{\phi_1} - \frac{x_{t-1} - m}{1 - \phi_1} \right) \rho_1(m, x_{t-1}, x_t, \phi_1, \lambda) \right) I_{1,t}^R.\end{aligned}\tag{13}$$

Note that

$$\begin{aligned}-\frac{x_{t-1}}{1 - \phi_1} &\leq \frac{m}{\phi_1} - \frac{x_{t-1} - m}{1 - \phi_1} \leq \frac{x_{t-1}}{\phi_1}, \\ -1 &\leq \frac{x_t - m}{\lambda} - 1 < \frac{x_t}{\lambda}.\end{aligned}$$

Since $\phi_1 \in (0, 1)$ and $\lambda \in (0, \infty)$, it is easy to get

$$\mathbb{E} \left(\frac{\partial^2}{\partial \lambda \partial \phi_1} \log P(x_{t-1}, x_t) \right) = \mathbb{E} \left(\frac{\partial^2}{\partial \phi_1 \partial \lambda} \log P(x_{t-1}, x_t) \right) < C_1 \cdot \mathbb{E} X_t^2 < \infty, \text{ (by Proposition 2.2).}$$

for some suitable constant C_1 . By the same arguments as above, it follows that

$$\mathbb{E} \left(\frac{\partial^2}{\partial \lambda \partial \phi_2} \log P(x_{t-1}, x_t) \right) = \mathbb{E} \left(\frac{\partial^2}{\partial \phi_2 \partial \lambda} \log P(x_{t-1}, x_t) \right) < C_2 \cdot \mathbb{E} X_t^2 < \infty, \text{ (by Proposition 2.2).}$$

for some suitable constant C_2 .

From the above discussions, we can get

$$\sqrt{n}(\hat{\theta}_{CML} - \theta_0) \xrightarrow{d} N(\mathbf{0}, \mathbf{J}^{-1}(\theta_0) \mathbf{I}(\theta_0) \mathbf{J}^{-1}(\theta_0)),$$

where $\mathbf{I}(\theta_0) = \mathbb{E} \left[\frac{\partial l_t(\theta)}{\partial \theta} \frac{\partial l_t(\theta)}{\partial \theta^T} \right]_{\theta_0}$, $\mathbf{J}(\theta_0) = \mathbb{E} \left[\frac{\partial^2 l_t(\theta)}{\partial \theta \partial \theta^T} \right]_{\theta_0}$. The proof of Theorem 3.2 is completed. \square

D-Ness algorithm We outline the precise procedures for applying the D-Ness algorithm to the BiNB-MTTINAR(1) model since we want to compare our suggested methods to the Ness algorithm. For a given λ , using standard least squares techniques, the sum of squared errors function is

$$S_n(r, \lambda) = \sum_{t=1}^n \left(X_t - \sum_{k=1}^2 \frac{\sum_{t=1}^n X_t X_{t-1} I_{k,t}(r) - \lambda \sum_{t=1}^n X_{t-1} I_{k,t}(r)}{\sum_{t=1}^n X_{t-1}^2 I_{k,t}(r)} \cdot X_{t-1} I_{k,t}(r) - \lambda \right)^2,$$

where $I_{1,t}(r) = I\{X_{t-1} \leq r\}$, $I_{2,t}(r) = I\{X_{t-1} > r\}$ are both functions with respect to r . Let

$$J_n(r, \lambda) = \sum_{t=1}^n \left(X_t - \frac{\sum_{t=1}^n X_t X_{t-1} - \lambda \sum_{t=1}^n X_{t-1}}{\sum_{t=1}^n X_{t-1}^2} \cdot X_{t-1} - \lambda \right)^2 - S_n(r, \lambda),$$

for a fixed λ , our aim is to estimate r_λ by maximizing $J_n(r, \lambda)$, i.e.,

$$\hat{r}_\lambda = \arg \max_{r \in [\underline{r}, \bar{r}]} J_n(r, \lambda). \quad (14)$$

Let $\underline{\lambda}$ and $\bar{\lambda}$ be some known lower and upper bounds of λ . We come to search for the final $\hat{r}_{CLS}^{(1)}$ by the following steps:

Step 1. Choose some appropriate positive integer L , let $\lambda(j) = \underline{\lambda} + \frac{j(\bar{\lambda} - \underline{\lambda})}{L}$, $j = 0, 1, \dots, L$.

Step 2. For each $j \in \{0, 1, \dots, L\}$, calculate $\hat{r}_{\lambda(j)}$ by (14).

Step 3. The final $\hat{r}_{CLS}^{(1)}$ is calculated by $\hat{r}_{CLS}^{(1)} = \arg \max_{0 \leq j \leq L} J_n(\hat{r}_{\lambda(j)}, \lambda(j))$. \square

Proof of Theorems 3.3 From the first partial derivative equal to 0, after some calculations, we obtain $\hat{\boldsymbol{\vartheta}}$ closed-form expressions as follows

$$\begin{aligned} \hat{\sigma}_1^2 &= \frac{\sum_{t=1}^n I_{1,t}^R \sum_{t=1}^n I_{1,t}^R V_t X_{t-1} - \sum_{t=1}^n I_{1,t}^R X_{t-1} \sum_{t=1}^n I_{1,t}^R V_t}{\sum_{t=1}^n I_{1,t}^R \sum_{t=1}^n I_{1,t}^R X_{t-1}^2 - (\sum_{t=1}^n I_{1,t}^R X_{t-1})^2}, \\ \hat{\sigma}_2^2 &= \frac{\sum_{t=1}^n I_{2,t}^R \sum_{t=1}^n I_{2,t}^R V_t X_{t-1} - \sum_{t=1}^n I_{2,t}^R X_{t-1} \sum_{t=1}^n I_{2,t}^R V_t}{\sum_{t=1}^n I_{2,t}^R \sum_{t=1}^n I_{2,t}^R X_{t-1}^2 - (\sum_{t=1}^n I_{2,t}^R X_{t-1})^2}, \\ \hat{b}_1 &= \frac{\sum_{t=1}^n I_{1,t}^R X_{t-1}^2 \sum_{t=1}^n I_{1,t}^R V_t - \sum_{t=1}^n I_{1,t}^R X_{t-1} \sum_{t=1}^n I_{1,t}^R V_t X_{t-1}}{\sum_{t=1}^n I_{1,t}^R \sum_{t=1}^n I_{1,t}^R X_{t-1}^2 - (\sum_{t=1}^n I_{1,t}^R X_{t-1})^2}, \\ \hat{b}_2 &= \frac{\sum_{t=1}^n I_{2,t}^R X_{t-1}^2 \sum_{t=1}^n I_{2,t}^R V_t - \sum_{t=1}^n I_{2,t}^R X_{t-1} \sum_{t=1}^n I_{2,t}^R V_t X_{t-1}}{\sum_{t=1}^n I_{2,t}^R \sum_{t=1}^n I_{2,t}^R X_{t-1}^2 - (\sum_{t=1}^n I_{2,t}^R X_{t-1})^2}. \end{aligned}$$

From the properties of Bernoulli, Geometric, Poisson random variables, there is

$$\begin{aligned} E(B_i - E(B_i))^4 &= (1 - \phi_1)^3 \phi_1 + 3(1 - \phi_1)^2 \phi_1^2 < \infty, \\ E(W_i - E(W_i))^4 &= \phi_2 + 10\phi_2^2 + 18\phi_2^3 + 8\phi_2^4 < \infty, \\ E(Z_{1,t} - E(Z_{1,t}))^4 &= \lambda + 3\lambda^2 < \infty, \\ E(Z_{2,t} - E(Z_{2,t}))^4 &= \lambda + 10\lambda^2 + 18\lambda^3 + 8\lambda^4 < \infty. \end{aligned}$$

It follows from Theorems 3.3 in Winnicki (1991) that $\hat{\boldsymbol{\vartheta}}$ is a consistent and asymptotically normal estimator of $\boldsymbol{\vartheta}$. The proof of Theorem 3.3 is completed. \square

References

- Amemiya, T., 1985. Advanced econometrics. *Harvard University Press: Cambridge*.
- Chan, W.S., Wong, A.C.S., Tong, H., 2004. Some nonlinear threshold autoregressive time series models for actuarial use. *North American Actuarial Journal*, 8, 37-61.

- Chen, C.W.S., Liu, F.C., So, M.K.P., 2011. A review of threshold time series models in finance. *Statistics and its Interface*, 4, 167-181.
- Wei, C., Scherer, L., Aleksandrov, B., Feld, M. 2019. Checking model adequacy for count time series by using Pearson residuals. *Journal of Time Series Econometrics*, 12, 20180018.
- Freeland, R.K., McCabe, B.P.M., 2004. Forecasting discrete valued low count time series. *International Journal of Forecasting*, 20, 427-434.
- Hansen, B.E., 2011. Threshold autoregression in economics. *Statistics and its Interface*, 4, 123-127.
- Kang, Y., Wang, D., Yang, K., 2021 A new INAR(1) process with bounded support for counts showing equidispersion, underdispersion and overdispersion. *Statistical Papers*, 62, 745-767.
- Karlsen, H., Tjøtheim, D., 1988. Consistent estimates for the NEAR (2) and NLAR (2) time series models. *Journal of the Royal Statistical Society: Series B (Methodological)*, 50, 313-320.
- Klimko, L.A., Nelson, P.I., 1978. On conditional least squares estimation for stochastic processes. *The Annals of Statistics*, 6, 629-642.
- Li, D., Tong, H., 2016. Nested sub-sample search algorithm for estimation of threshold models. *Statistica Sinica*, 26, 1543-1554.
- Li, H., Yang, K., Zhao, S., et al., 2018. First-order random coefficients integer-valued threshold autoregressive processes. *AStA Advances in statistical analysis*, 102, 305-331.
- Maiti, R., Biswas, A., 2017. Coherent forecasting for stationary time series of discrete data. newblock *AStA Advances in Statistical Analysis*, 99, 337-365.
- Möller, T.A., Silva, M.E., Wei, C.H., et al., 2016. Self-exciting threshold binomial autoregressive processes. *AStA Advances in Statistical Analysis*, 100, 369-400.
- Möller, T.A., Wei, C.H., 2015. Threshold models for integer-valued time series with infinite or finite range. *Stochastic models, statistics and their applications*, Springer Proceedings in Mathematics & Statistics, 122, 327-334.
- Monteiro, M., Scotto, M.G. and Pereira, I., 2012. Integer-valued self-exciting threshold autoregressive processes. *Communications in Statistics - Theory and Methods*, 41, 2717-2737.
- Nastić A.S., Ristić M.M., Janjić A.D., 2017. A mixed thinning based geometric INAR (1) model. *Filomat*, 31, 4009-4022.
- Ristić, M.M., Bakouch, H.S., Nastić, A.S., 2009. A new geometric first-order integer-valued autoregressive (NGINAR(1)) process. *Journal of Statistical Planning and Inference*, 139, 2218-2226.

- Ristić, M.M., Nastić, A.S., Miletić, Ilić A.V., 2013. A geometric time series model with dependent Bernoulli counting series. *Journal of Time Series Analysis*, 34, 466-476.
- Steutel, F., Van Harn, K., 1979. Discrete analogues of self-decomposability and stability. *The Annals of Probability*, 7, 893-899.
- Tong, H., 1978. On a threshold model. In C. H. Chen (ed.). *Pattern Recognition and Signal Processing*.
- Tong, H., 1983. *Threshold Models in Nonlinear Time Series Analysis*. Lecture Notes in Statistics, Springer-Verlag, New York.
- Wang, C., Liu, H., Yao, J., et al., 2014. Self-excited threshold Poisson autoregression. *Journal of the American Statistical Association*, 109, 776-787.
- Winnicki J., 1991. Estimation of the variances in the branching process with immigration. *Probability Theory and Related Fields*, 88, 77-106.
- Yang, K., Wang, D., Jia, B., et al., 2018. An integer-valued threshold autoregressive process based on negative binomial thinning. *Statistical Papers*, 59, 1131-1160.
- Yang, K., Li, H., Wang, D., 2018. Estimation of parameters in the self-exciting threshold autoregressive processes for nonlinear time series of counts. *Applied Mathematical Modelling*, 57, 226-247.
- Zhang, Q., Wang, D., Fan, X., 2020. A negative binomial thinning-based bivariate INAR (1) process. *Statistica Neerlandica*, 74, 517-537.
- Zhang, C., Wang, D., Yang, K., Li, H., et al., 2022. Generalized Poisson integer-valued autoregressive processes with structural changes. *Journal of Applied Statistics*, 49, 2717-2739.
- Zhu, F., 2012. Zero-inflated Poisson and negative binomial integer-valued GARCH models. *Journal of Statistical Planning and Inference*, 142, 826-839.